Lectures on Heavy-Flavor Probes of Quark-Gluon Plasma

Min He

Nanjing Univ. of Sci. & Tech., Nanjing, China

Lecture II

Open heavy flavor production in AA collisions

- Simulation of HQ diffusion in QGP: Langevin vs Boltzmann
- Microscopic interactions of HQs in QGP
- HQ Hadronization
- Heavy hadron interaction in hot hadronic medium
- Phenomenology

Heavy flavor transport as probes of QGP

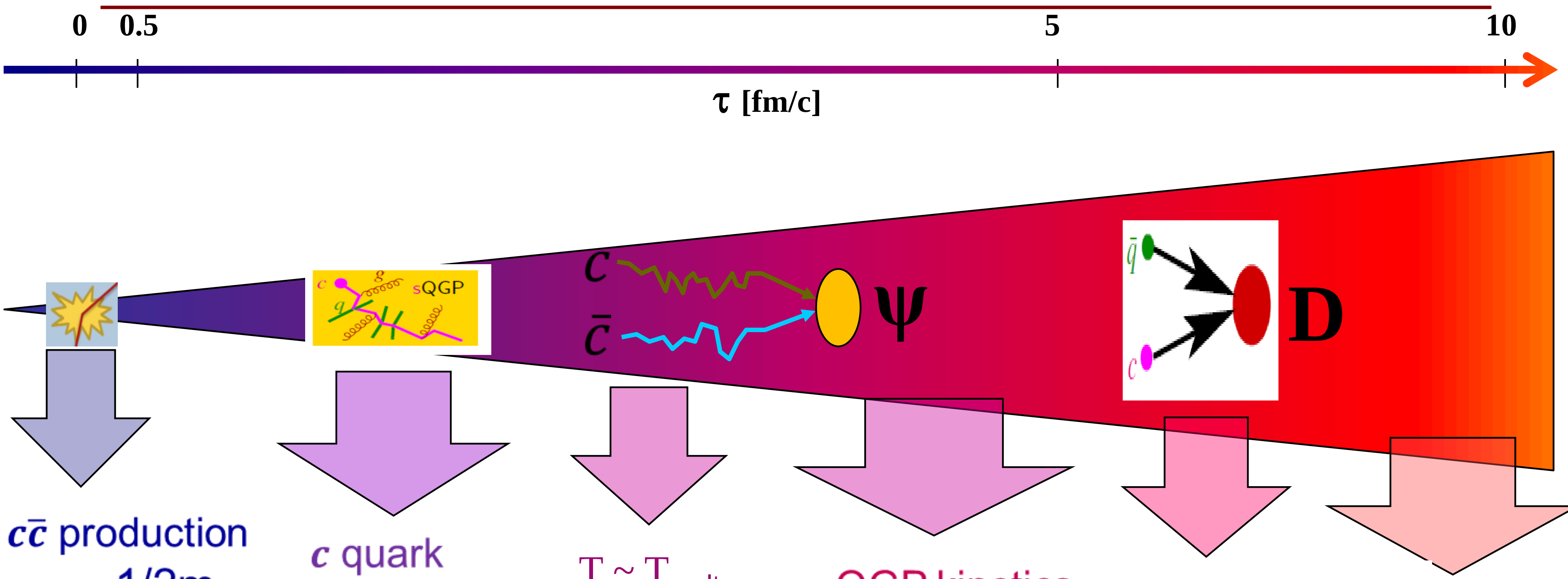

$c\bar{c}$ production
τ_{hard}~1/2m$_c$,
buildup of ψ
wave packet
τ_ψ ~1 fm/c

c quark
Brownian
diffusion
in QGP
τ_c^{eq} ~5 fm/c

$T \sim T_{melt}$
onset of
quarkonium
regeneration

QGP kinetics
$c + \bar{c} \leftrightarrow \psi$
$\tau_\psi^{eq} \sim 1/\Gamma_\psi$

$T \sim T_c$
hadronization:
$c+q \rightarrow D$
$c+q+q \rightarrow \Lambda_c$

hadronic
diffusion

HQ evolution in hot QCD medium

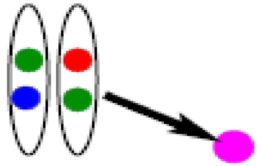

- c-cbar (b-bbar) produced in pairs in early hard processes t~$1/2m_Q$, calculable via pQCD

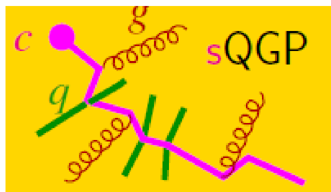

- single HQs diffusion and rescattering in sQGP via elastic or inelastic/radiative interactions, simulated by Boltzmann/Langevin equations

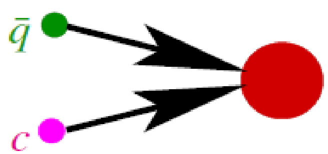

- HQ hadronization via coalescence c+qbar→D, c+q+q→Λ_c, or independent fragmentation

- D, Λ_c further diffusion in HRG via hadronic interactions with bulk hadrons

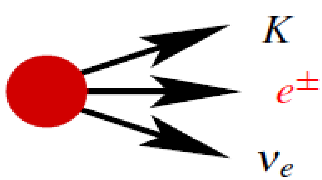

- D, Λ_c decay long after freezeout of the system via weak interactions (semileptonic or hadronic e.g. B→J/ψ+K (nonprompt J/ψ))

HQ transport in QGP: Boltzmann eq.

- describe heavy-quark scattering in the QGP by (semi-)classical transport equation
- $f_Q(t, \vec{x}, \vec{p})$: phase-space distribution of heavy quarks
- equation of motion for HQ-fluid cell at time t at $(\vec{p}, \vec{x})$:

$$\mathrm{d}f_Q = \mathrm{d}t \left(\frac{\partial}{\partial t} + \vec{v} \frac{\partial}{\partial \vec{x}} + \vec{F} \cdot \frac{\partial}{\partial \vec{p}} \right) f_Q$$

  - change of phase-space distribution with time (non-equilibrium)
  - drift of HQ-fluid cell with velocity $\vec{v} = \vec{p}/E_{\vec{p}}$, $E_{\vec{p}} = \sqrt{m_Q^2 + \vec{p}^2}$
  - change of momentum with mean-field force, $\vec{F}$
- change must be due to collisions with surrounding medium

$$\mathrm{d}f_Q = C[f_Q] = \int \mathrm{d}^3\vec{k} [\underbrace{w(\vec{p}+\vec{k}, \vec{k}) f_Q(t, \vec{x}, \vec{p}+\vec{k})}_{\text{gain}} - \underbrace{w(\vec{p}, \vec{k}) f_Q(t, \vec{x}, \vec{p})}_{\text{loss}}]$$

  - $w(\vec{p}, \vec{k})$: transition rate for collision of a heavy quark with momentum, $\vec{p}$ with a heat-bath particle with momentum transfer, $\vec{k}$

Boltzmann equation (2→2)

- relation to cross sections of microscopic scattering processes
- e.g., elastic scattering of heavy quark with light quarks

$$w(\vec{p},\vec{k}) = \gamma_q \int \frac{\mathrm{d}^3\vec{q}}{(2\pi)^3} f_q(\vec{q}) v_{\text{rel}}(\vec{p},\vec{q} \to \vec{p}-\vec{k},\vec{q}+\vec{k}) \frac{\mathrm{d}\sigma}{\mathrm{d}\Omega}$$

- $\gamma_q = 2 \times 3 = 6$: spin-color-degeneracy factor
- $v_{\text{rel}} := \sqrt{(p \cdot q)^2 - (m_Q m_q)^2}/(E_Q E_q)$; covariant relative velocity
- in terms of invariant matrix element

$$\begin{aligned} C[f_Q] =& \frac{1}{2E_Q} \int \frac{\mathrm{d}^3\vec{q}}{(2\pi)^3 2E_q} \int \frac{\mathrm{d}^3\vec{p}\,'}{(2\pi)^3 2E_p'} \int \frac{\mathrm{d}^3\vec{q}\,'}{(2\pi)^3 2E_q'} \\ & \times \frac{1}{\gamma_Q} \sum_{c,s} \left|\mathcal{M}_{(\vec{p}\,',\vec{q}\,') \leftarrow (\vec{p},\vec{q})}\right|^2 \\ & \times (2\pi)^4 \delta^{(4)}(p+q-p'-q')[f_Q(\vec{p}\,')f_q(\vec{q}\,') - f_Q(\vec{p})f_q(\vec{q})] \end{aligned}$$

  - $\vec{p}$, $\vec{q}$ ($\vec{p}\,'$, $\vec{q}\,'$) initial (final) momenta of heavy and light quark
  - momentum transfer: $\vec{k} = \vec{q}\,' - \vec{q} = \vec{p} - \vec{p}\,'$

Reduction to Fokker-Planck equation

- heavy quarks $\leftrightarrow$ light quarks/gluons: momentum transfers small
- $w(\vec{p}+\vec{k},\vec{k})$: peaked around $\vec{k}=0$
- expansion of collision term around $\vec{k}=0$

$$w(\vec{p}+\vec{k},\vec{k})f_Q(\vec{p}+\vec{k},\vec{k}) \simeq w(\vec{p},\vec{k})f_Q(\vec{p}) + \vec{k}\cdot\frac{\partial}{\partial\vec{p}}[w(\vec{p},\vec{k})f_Q(\vec{p})] + \frac{1}{2}k_i k_j \frac{\partial^2}{\partial\vec{p}_i\vec{p}_k}[w(\vec{p},\vec{k})f_Q(\vec{p})]$$

- collision term

$$C[f_Q] = \int \mathrm{d}^3\vec{k}\left[k_i\frac{\partial}{\partial p_i} + \frac{1}{2}\frac{\partial^2}{\partial p_i \partial p_j}\right][w(\vec{p},\vec{k})f_Q(\vec{p})].$$

Reduction to Fokker-Planck equation

- Boltzmann equation $\Rightarrow$ simplifies to Fokker-Planck equation

$$\partial_t f_Q(t,\vec{x},\vec{p}) + \frac{\vec{p}}{E_{\vec{p}}}\cdot\frac{\partial}{\partial\vec{x}} f_Q(t,\vec{x},\vec{p}) = \frac{\partial}{\partial p_i}\left\{A_i(\vec{p}) f_Q(t,\vec{x},\vec{p}) + \frac{\partial}{\partial p_j}\left[B_{ij}(\vec{p}) f_Q(t,\vec{p})\right]\right\}$$

- with drag and diffusion coefficients

$$A_i(\vec{p}) = \int \mathrm{d}^3\vec{k}\, k_i w(\vec{p},\vec{k}), \quad B_{ij}(\vec{p}) = \frac{1}{2}\int \mathrm{d}^3\vec{k}\, k_i k_j w(\vec{p},\vec{k})$$

- equilibrated light quarks and gluons: coefficients in heat-bath frame
- matter homogeneous and isotropic

$$A_i(\vec{p}) = A(p)p_i, \quad B_{ij}(\vec{p}) = B_0(p)P_{ij}^{\perp} + B_1(p)P_{ij}^{||}$$

$$\text{with} \quad P_{ij}^{||}(\vec{p}) = \frac{p_i p_j}{\vec{p}^2}, \quad P_{ij}^{\perp}(\vec{p}) = \delta_{ij} - \frac{p_i p_j}{\vec{p}^2}$$

$$\begin{aligned} A_i(\boldsymbol{p}) = {} & \frac{1}{2E(\boldsymbol{p})}\int\frac{d^3\boldsymbol{q}}{(2\pi)^3 2E(\boldsymbol{q})}\int\frac{d^3\boldsymbol{q}'}{(2\pi)^3 2E(\boldsymbol{q}')} \\ & \times \int\frac{d^3\boldsymbol{p}'}{(2\pi)^3 2E(\boldsymbol{p}')}\frac{1}{\gamma}\sum|\mathcal{M}|^2 \hat{f}(\boldsymbol{q}) \\ & (2\pi)^4\delta^4(p+q-p'-q')\,[(\boldsymbol{p}'-\boldsymbol{p})_i] \\ \equiv {} & \langle\langle(\boldsymbol{p}'-\boldsymbol{p})_i\rangle\rangle; \end{aligned}$$

$$B_{ij}(\boldsymbol{p}) = \frac{1}{2}\langle\langle(\boldsymbol{p}'-\boldsymbol{p})_i(\boldsymbol{p}'-\boldsymbol{p})_j\rangle\rangle.$$

A,B can be calculated from scattering amplitudes, but are not independent of each other!

Einstein relation & equilibrium limit

- FP equation cast into a continuity equation in momentum space

$$\frac{\partial f_Q(t,\boldsymbol{p})}{\partial t} + \frac{\partial}{\partial p_i} S_i(t,\boldsymbol{p}) = 0. \quad S_i(t,\boldsymbol{p}) = -\left\{ A_i(\boldsymbol{p}) f(t,\boldsymbol{p}) + \frac{\partial}{\partial p_j} [B_{ij}(\boldsymbol{p}) f(t,\boldsymbol{p})] \right\}$$

- In the equilibrium limit ➔ Boltzmann-Juttner distribution

$$f_{\rm eq}(p,T) = N \exp[-E(p)/T] \qquad E(p) = \sqrt{p^2+m^2}$$

particle current/flux vanishes S_i=0 ➔ fluctuation-dissipation theorem between drag and diffusion coefficient

$$A_i(\boldsymbol{p},T) = B_{ij}(\boldsymbol{p},T)\frac{1}{T}\frac{\partial E(p)}{\partial p_j} - \frac{\partial B_{ij}(\boldsymbol{p},T)}{\partial p_j}$$

- Non-relativistic limit with diagonal diffusion

$$A(p) = \frac{1}{E(p)}\left(\frac{D[E(p)]}{T} - \frac{\partial D[E(p)]}{\partial E}\right) \qquad B_0(p) = B_1(p) = D(p)$$

in the non-relativistic limit, D(p)=D, Γ(p)=γ ➔ Einstein relation: $D = m\gamma T$

- Analytical solution

$$f(p,t) = \left[\frac{\gamma}{2\pi D}(1-e^{-2\gamma t})\right]^{-1/2} \times \exp\left[-\frac{\gamma}{2D}\frac{(p-p_0 e^{-\gamma t})^2}{1-e^{-2\gamma t}}\right]$$

- drag on mean momentum: $\langle p \rangle = p_0 e^{-\gamma t}$
- diffusion in momentum & coordinate space:

$$\langle p^2 \rangle - \langle p \rangle^2 = \frac{D}{\gamma}(1-e^{-2\gamma t}) \qquad \langle x^2 \rangle - \langle x \rangle^2 \sim \frac{2D}{m^2\gamma^2} t = 2D_s t$$

$$D_s = \frac{T}{m_Q \gamma} = \frac{T^2}{D}$$

Langevin equation

- FP equation stochastically realized by Langevin equation

$$dx_j = \frac{p_j}{E}dt,$$

$$dp_j = -\Gamma(p,T)p_j dt + \sqrt{dt}C_{jk}(\boldsymbol{p}+\xi d\boldsymbol{p},T)\rho_k$$

$$\longrightarrow$$

$$\frac{\partial f(t,\boldsymbol{p})}{\partial t} = \frac{\partial}{\partial p_j}\left[\left(\Gamma(p)p_j - \xi C_{lk}(\boldsymbol{p})\frac{\partial C_{jk}(\boldsymbol{p})}{\partial p_l}\right)f(t,\boldsymbol{p})\right] + \frac{1}{2}\frac{\partial^2}{\partial p_j \partial p_k}[C_{jl}(\boldsymbol{p})C_{kl}(\boldsymbol{p})f(t,\boldsymbol{p})]. \quad (10)$$

Γ(p,T) --- deterministic drag/friction force;

C_{jk}--- stochastically fluctuating force with independent Gaussian noise $P(\boldsymbol{\rho}) = (2\pi)^{-3/2}e^{-\boldsymbol{\rho}^2/2}$

no correlation at different times $\langle F_j(t)F_k(t')\rangle = C_{jl}C_{kl}\delta(t-t')$

- Pre-point scheme: $\xi = 0$

$$dx_j = \frac{p_j}{E}dt,$$

$$dp_j = -\Gamma(p)p_j dt + \sqrt{2dt\,D(p)}\rho_j$$

with equilibrium condition: $\Gamma(p) = \frac{1}{E(p)}\left(\frac{D[E(p)]}{T} - \frac{\partial D[E(p)]}{\partial E}\right) = A(p)$

➔ F-P equation: $\frac{\partial}{\partial t}f(t,\boldsymbol{p}) = \frac{\partial}{\partial p_i}\left\{\Gamma(p)p_i f(t,\boldsymbol{p}) + \frac{\partial}{\partial p_i}[D(p)f(t,\boldsymbol{p})]\right\}$

- Post-point scheme: $\xi = 1$

$$dx_j = \frac{p_j}{E}dt,$$

$$dp_j = -\Gamma(p)p_j dt + \sqrt{2dt\,D(|\boldsymbol{p}+d\boldsymbol{p}|)}\rho_j$$

with equilibrium condition: $D[E(p)] = \Gamma(p)E(p)T,$

$$\Gamma(p) = A(p) + \frac{1}{E(p)}\frac{\partial D[E(p)]}{\partial E}$$

➔ F-P equation: $\frac{\partial}{\partial t}f(t,\boldsymbol{p}) = \frac{\partial}{\partial p_i}\left\{\Gamma(p)p_i f(t,\boldsymbol{p}) + D(p)\frac{\partial}{\partial p_i}f(t,\boldsymbol{p})\right\}$

In terms of A and D, the F-P equations in pre- and post-points are the same!

MH et al., PRE88,032138(2013)

Langevin eqs. are not covariant! So updates of x, p need to be done in fluid rest frame when there's collective flow!

Equilibrium limit check

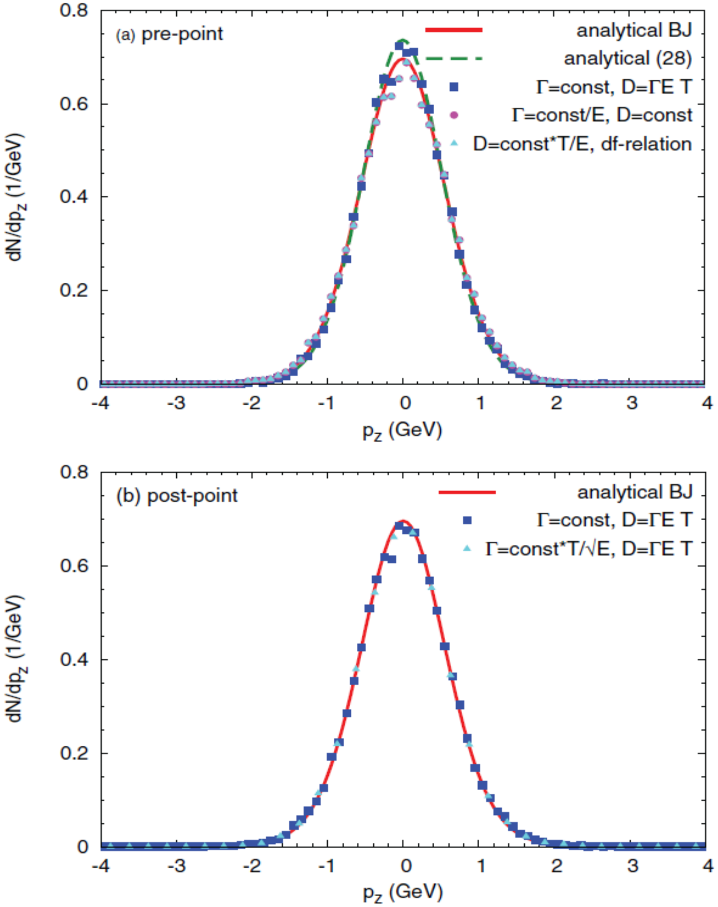

FIG. 1. (Color online) Distribution dN/dp_z from Langevin simulations for heavy quarks with mass $m = 1.5$ GeV, diffusing in a static medium at temperature $T = 0.18$ GeV, compared to calculations with the corresponding analytical phase-space distributions: (a) prepoint Langevin scheme; (b) postpoint Langevin scheme. See text for more details.

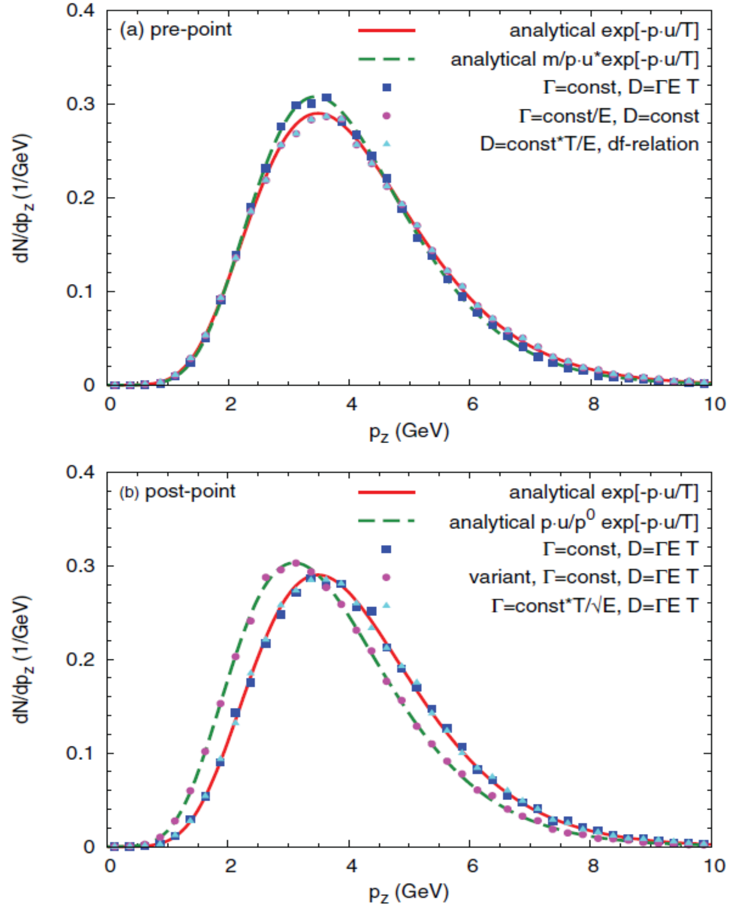

FIG. 2. (Color online) Langevin simulation results for heavy quarks $(m = 1.5$ GeV) diffusing in a flowing medium $(T = 0.18$ GeV, $v_z = 0.9)$ compared to calculations with analytical phase-space distributions: (a) prepoint Langevin scheme; (b) postpoint Langevin scheme. The distribution obtained with a variant of the postpoint scheme and the corresponding blast-wave distribution are also shown. See text for more details.

Equilibrium limit check (elliptic fireball)

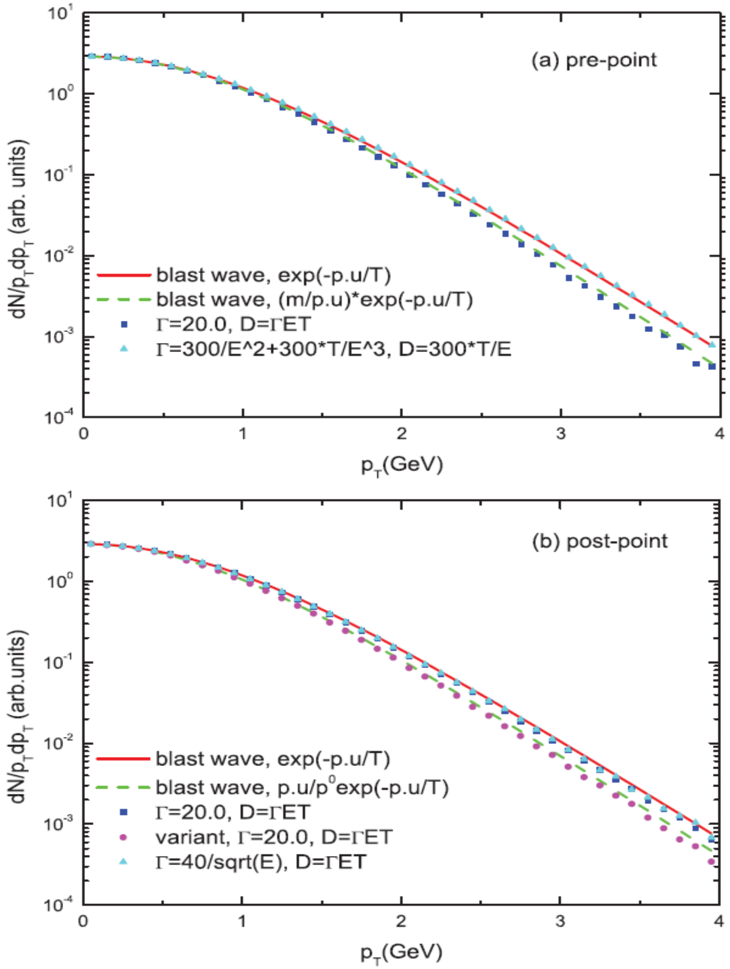

FIG. 3. (Color online) Langevin simulation of the p_T spectrum of a heavy quark ($m = 1.5$ GeV) diffusing in a fireball ($T_i = 0.33$ GeV, $T_f = 0.18$ GeV), compared to the direct blast-wave calculations. (a) Prepoint Langevin scheme; (b) postpoint Langevin scheme. See text for more details.

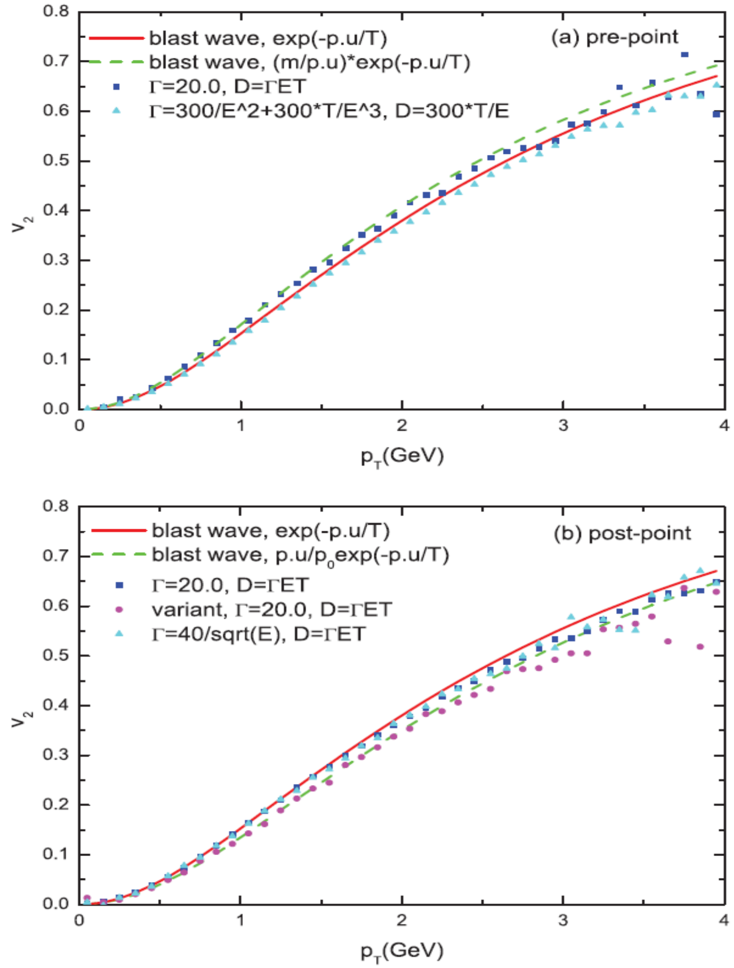

FIG. 4. (Color online) Langevin simulation results for $v_2(p_T)$ for a heavy quark ($m = 1.5$ GeV) diffusing in a QGP ($T_f = 0.18$ GeV) compared to direct blast-wave calculations with the flow field and temperature of the background medium (fireball). (a) Prepoint Langevin scheme; (b) postpoint Langevin scheme.

Full Boltzmann implementation

- Catania group: quasi-particles for bulk fitted to lattice-EoS + HQ elastic scattering

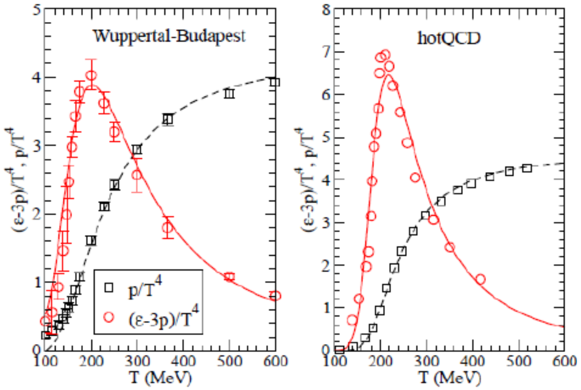

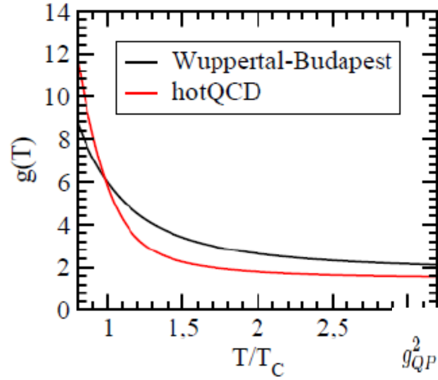

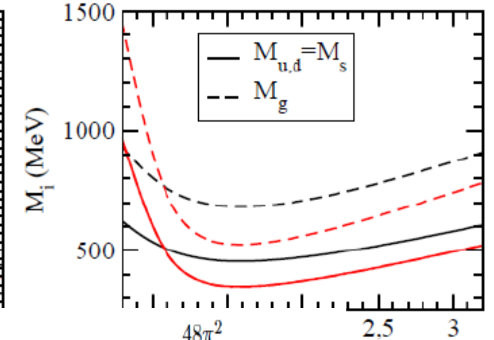

$$g^2_{QP}(T) = \frac{48\pi^2}{(11N_c - 2N_f)\ln\left[\lambda\left(\frac{T}{T_c} - \frac{T_s}{T_c}\right)\right]^2}$$

Plumari et al., PRD, 84, 094004 (2011)

$$p^\mu \partial_\mu f(x,p) = C_{22}$$

Das et al., PRC90, 044901(2014)

$$C_{22} = \frac{1}{2E_1}\int\frac{d^3p_2}{(2\pi)^3 2E_2}\frac{1}{\nu}\int\frac{d^3p'_1}{(2\pi)^3 2E'_1}\frac{d^3p'_2}{(2\pi)^3 2E'_2} f'_1 f'_2 |\mathcal{M}_{1'2'\to 12}|^2 (2\pi)^4 \delta^{(4)}(p'_1 + p'_2 - p_1 - p_2)$$
$$- \frac{1}{2E_1}\int\frac{d^3p_2}{(2\pi)^3 2E_2}\frac{1}{\nu}\int\frac{d^3p'_1}{(2\pi)^3 2E'_1}\frac{d^3p'_2}{(2\pi)^3 2E'_2} f_1 f_2 |\mathcal{M}_{12\to 1'2'}|^2 (2\pi)^4 \delta^{(4)}(p_1 + p_2 - p'_1 - p'_2)$$

- Similarly by (Q)LBT with both elastic+radiative collisions: $p_1 \cdot \partial f_1(x_1, p_1) = E_1(C_{\rm el} + C_{\rm inel}),$

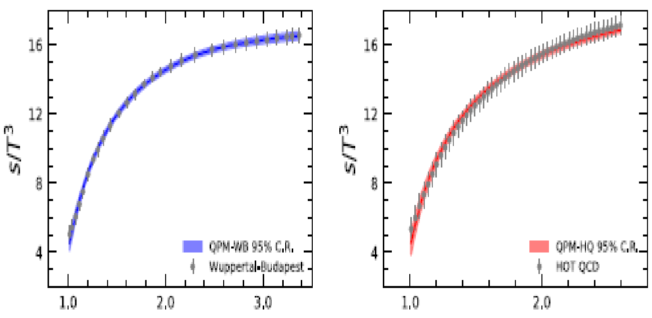

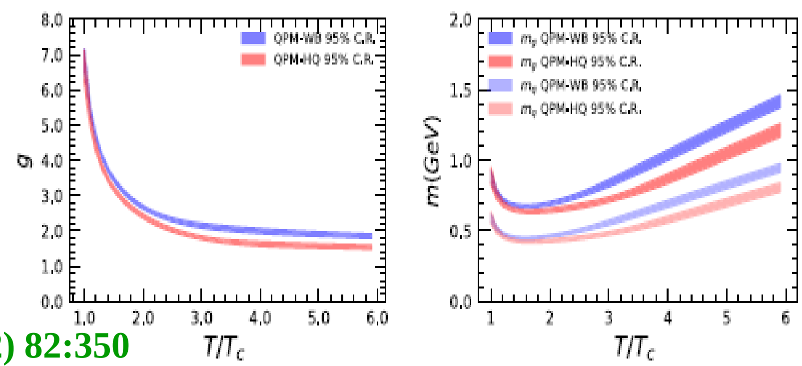

Liu et al, Eur. Phys. J. C (2022) 82:350

HQ scattering in QGP: pQCD

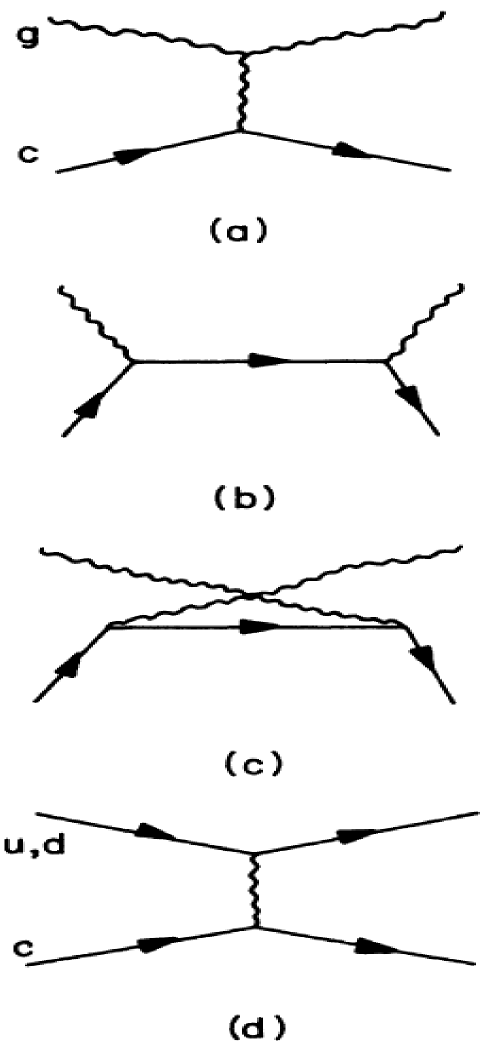

Svetitski, PRD37, 2484(1988)

$$\sum |\mathcal{M}_a|^2 = 3072\pi^2\alpha_s^2 \frac{(m^2-s)(m^2-u)}{(t-\mu^2)^2},$$

$$\sum |\mathcal{M}_b|^2 = \tfrac{2048}{3}\pi^2\alpha_s^2 \frac{(m^2-s)(m^2-u)-2m^2(m^2+s)}{(m^2-s)^2}$$

$$\sum |\mathcal{M}_c|^2 = \tfrac{2048}{3}\pi^2\alpha_s^2 \frac{(m^2-u)(m^2-s)-2m^2(m^2+u)}{(m^2-u)^2}$$

$$\sum \mathcal{M}_a\mathcal{M}_b^* = \sum \mathcal{M}_b\mathcal{M}_a^* = 768\pi^2\alpha_s^2 \frac{(m^2-s)(m^2-u)+m^2(u-s)}{(t-\mu^2)(m^2-s)},$$

$$\sum \mathcal{M}_a\mathcal{M}_c^* = \sum \mathcal{M}_c\mathcal{M}_a^* = 768\pi^2\alpha_s^2 \frac{(m^2-u)(m^2-s)+m^2(s-u)}{(t-\mu^2)(m^2-u)},$$

$$\sum \mathcal{M}_b\mathcal{M}_c^* = \sum \mathcal{M}_c\mathcal{M}_b^* = \tfrac{256}{3}\pi^2\alpha_s^2 \frac{m^2(t-4m^2)}{(m^2-u)(m^2-s)}$$

for gluon scattering, and

$$\sum |\mathcal{M}_d|^2 = 256N_f\pi^2\alpha_s^2 \frac{(m^2-s)^2+(m^2-u)^2+2m^2t}{(t-\mu^2)^2}$$

- t-channel scattering dominates, regularized by gluon screening mass $\mu_D \sim gT$

LO-pQCD is far from enough

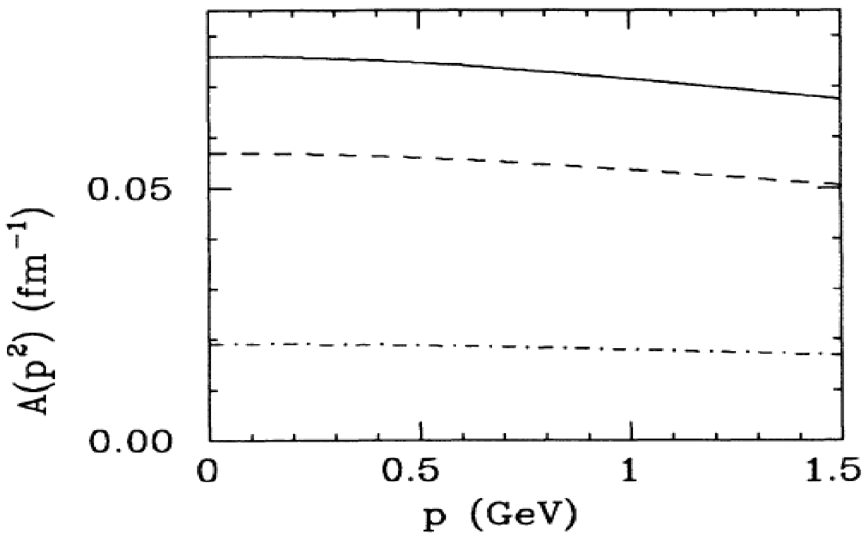

FIG. 2. Drag coefficient $A(p^2)$ at temperature $T=200$ MeV, assuming QCD coupling $\alpha_s=0.6$ and Debye screening mass $\mu=200$ MeV. The dashed-dotted curve is the contribution of quark and antiquark scattering, the dashed curve that of gluon scattering, and the solid line the sum of the two.

Svetitski, PRD37, 2484(1988)

- Here, α_s=0.6, μ_D=200 MeV, A ∝ α_s^2. If using more realistic α_s~0.3, A(p=0,T=200 MeV) ~0.02/fm ➔ need △t=1/A=50 fm/c for c-quark thermalization >> QGP lifetime

- LO-pQCD t-channel dominated by forward scattering, dσ/dΩ~1/θ^4, not efficient for momentum isotropilization/thermalization ➔ resonant scattering more efficient

Variants of LO-pQCD/Born diagram

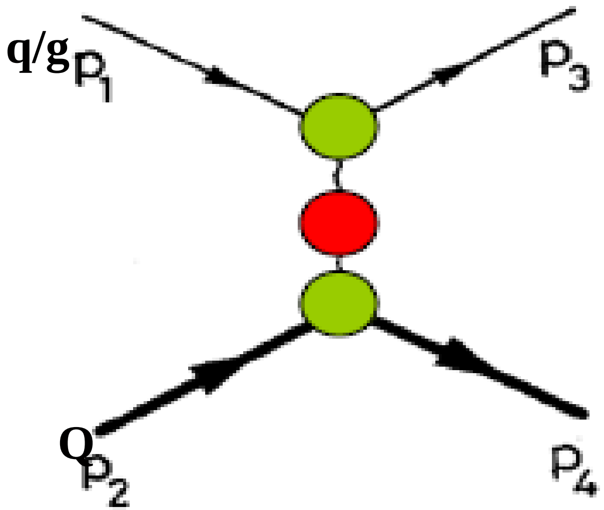

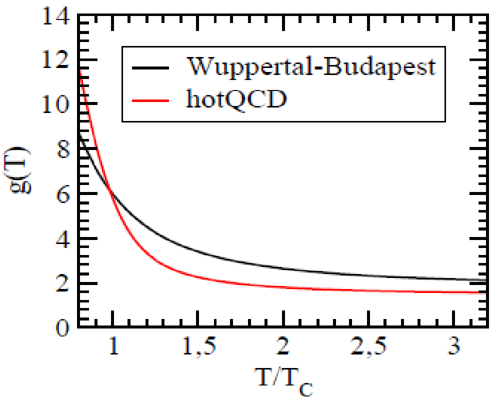

$$\frac{\alpha}{t} \rightarrow \frac{\alpha}{t-\mu^2} \rightarrow \frac{\alpha_{eff}}{t-\kappa m_D^2(T)}$$

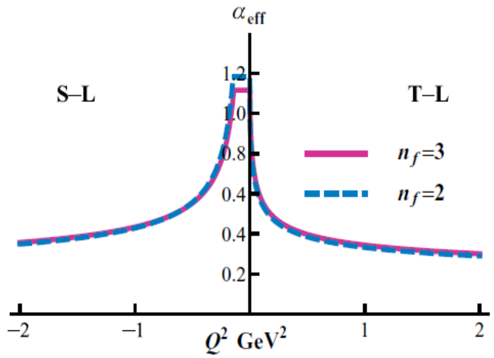

- Nantes group: reduced screening κ~ 0.11 to fit e-loss ➔ matrix element squared much enhanced (t<0) **Gossiaux et al., PRC 79, 044906 (2009)**

- Nantes/Catania group: quasi-particles with running/effective coupling const. α_{eff} ~1 at low T and/or low Q^2 ➔ inconsistent with LO approximation **Das et al., PRC90, 044901(2014)**

Dependence of charm drag on screening mass

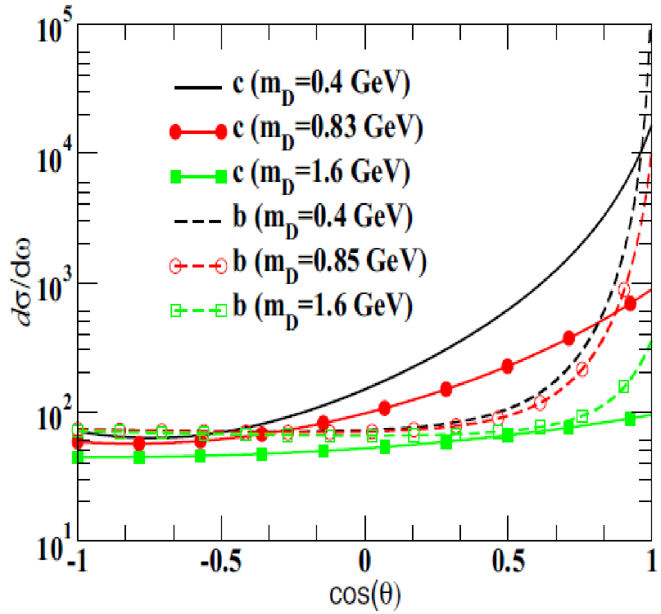

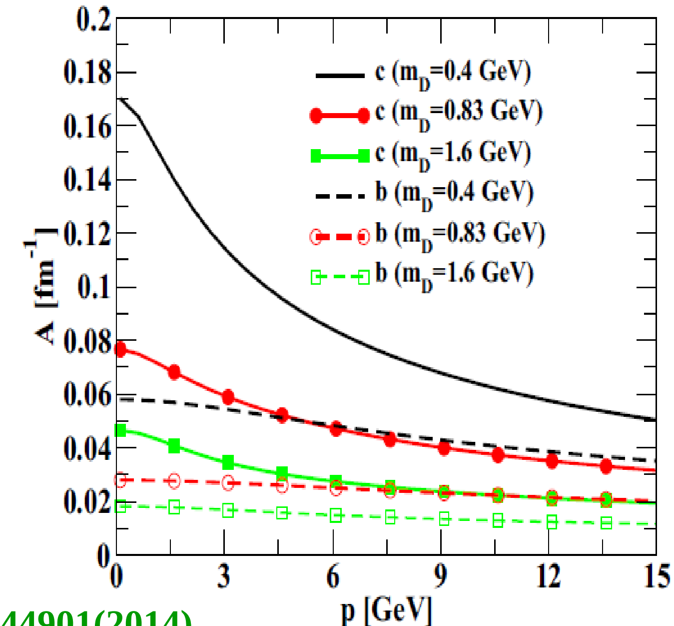

Das et al., PRC90, 044901(2014)

FIG. 1. (Color online) Angular dependence of the cross section for different values of m_D for charm quarks (solid lines) and for bottom quarks (dashed lines).

FIG. 3. (Color online) Variation of drag coefficients with p at $T =$ 400 MeV for different values of m_D.

- smaller m_D ➔ more forward LO-pQCD
- Matrix element squared increases so does thermal relaxation rate

Boltzmann vs Langevin using LO-pQCD

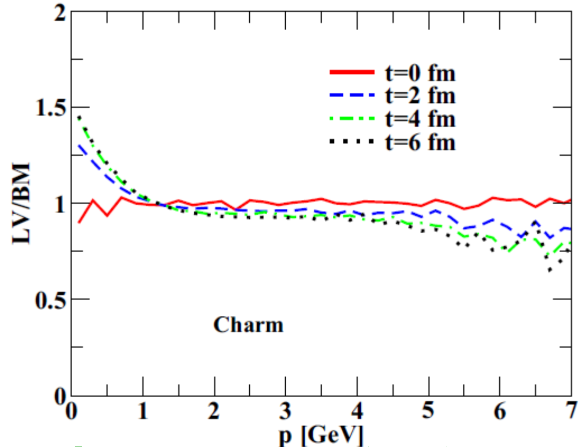

Das et al., PRC90, 044901(2014)

FIG. 6. (Color online) Ratio between the Langevin (LV) and Boltzmann (BM) spectra for charm quark as a function of momentum for $m_D = 0.4\,\mathrm{GeV}$ a

- At high p_T, Gauss distribution of e-loss underlying Langevin becomes less accurate ➔ deviation from full Boltzmann
- Charm quark R_{AA} is ~25% smaller from Langevin than Boltzmann at high p_T while v2 from Langevin a bit larger
- Discrepancies between Lagevin vs Boltzmann vanishes for bottom

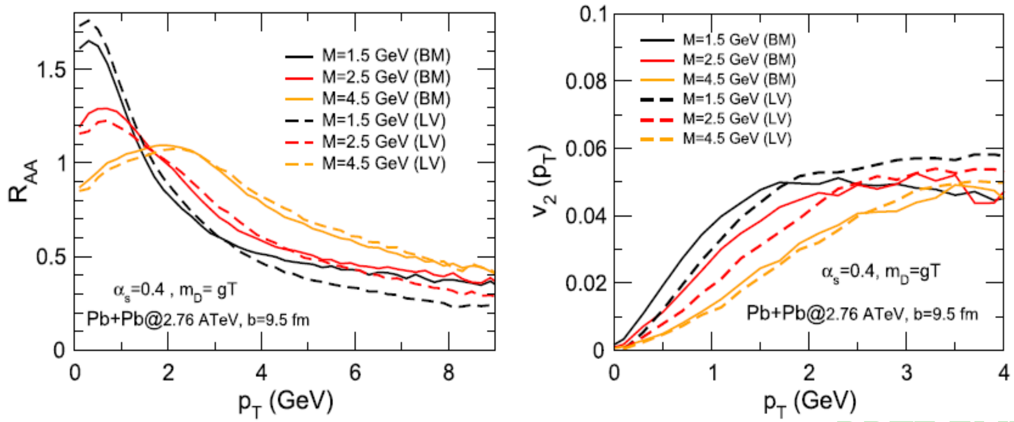

RRTF-EMMI, NPA979(2018)21-86

Fig. 24. Nuclear modification factor (left panel) and elliptic flow (right panel) for heavy quarks in semi-central Pb+Pb($\sqrt{s_{NN}} = 2.76$ TeV) collisions (at $b = 9.5$ fm) for different values of the HQ mass, M_Q (indicated by the different line colors), in a Boltzmann (solid lines) and in a Langevin approach (dashed lines).

pQCD: NLO

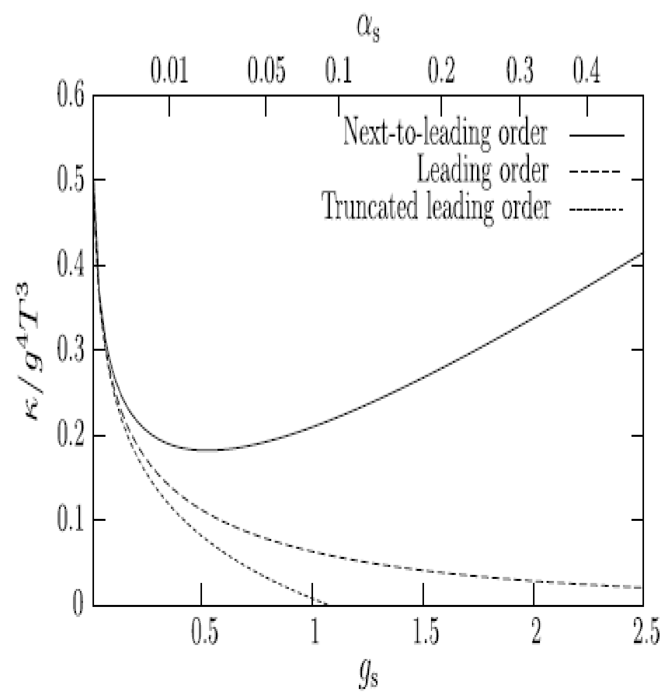

Caron-Huot & Moore, JHEP02(2008)081

Fig. 20. Comparison of leading and next-to-leading order inverse heavy-quark diffusion coefficient, $\kappa/T^3 = 2/(\mathcal{D}_s T)$, scaled by the leading-order coupling constant dependence. The subleading corrections are large even at coupling values usually considered to be very small.

- NLO >> LO ➔ poor convergence!

Non-perturbative effects

- Large running coupling at small Q^2 in LO-pQCD/Born diagram with one-gluon exchange ➔ strong Coulomb potential at large distance
- But at large distance, Q-Qbar potential is linear-confining term (in vacuum: $V(r) = -\frac{4}{3}\frac{\alpha_s}{r} + \sigma r$)
- At finite T (<2*Tc) significant remnants linear part in Q-Qbar free energy [yet not potential]
  ➔ residual confining force may be important for HQ interactions in QGP
  ➔ non-perturbative potential model needed!

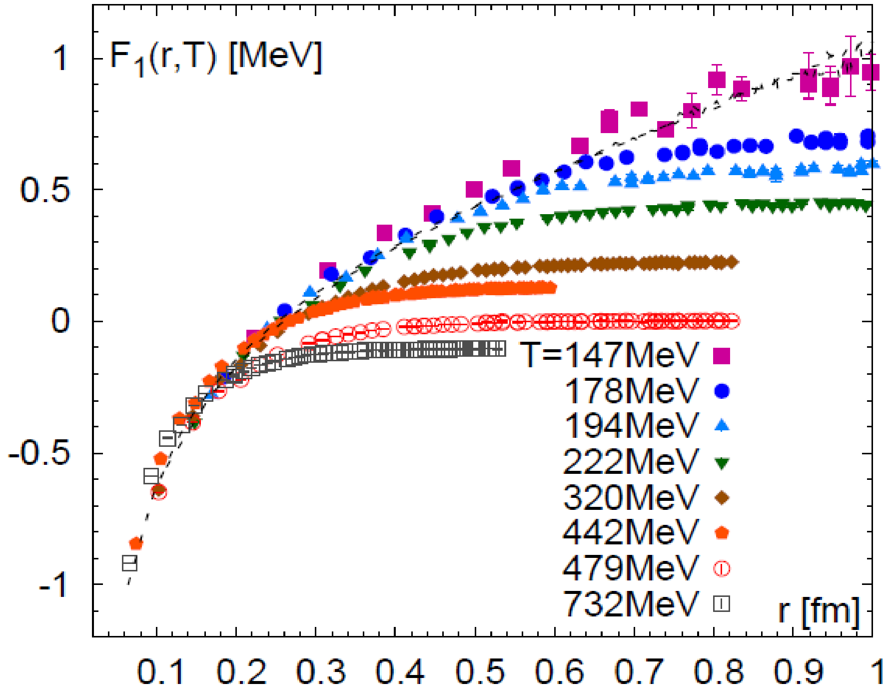

$$\exp(-F_1(r,T)/T) = \frac{1}{N}\langle \mathrm{Tr}[L^\dagger(x)L(y)]\rangle.$$

- If there's only Coulomb➔ F<0
- F>0 for T<2*T_c, remnant of linear confining term

T-matrix resuming HQ potential

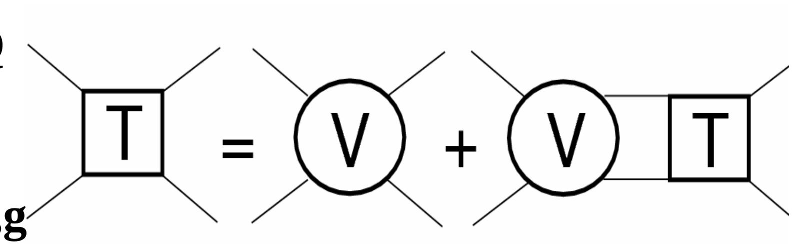

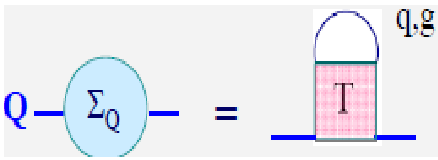

- 4D Bethe-Salpeter ➔ 3D Lippmann-Schwinger with relativistic corrections

$$
\begin{aligned}
&T_{l,a}(E;q',q) \\
&\quad = \mathcal{V}_{l,a}(q',q) + \frac{2}{\pi}\int_0^\infty dk\, k^2\, \mathcal{V}_{l,a}(q',k) \\
&\quad\quad \times G_{12}(E;k)\, T_{l,a}(E;k,q)\{1 - n_F[\omega_1(k)] - n_F[\omega_2(k)]\}
\end{aligned}
$$

$$
G_{12}^{\mathrm{Th}}(E;q) = \frac{m(q)}{E - \omega^q(q) - \omega^Q(q) - \Sigma_q - \Sigma_Q},
$$

$$
G_{12}^{\mathrm{BbS}}(E;q) = \frac{2\,m(q)\,(\omega^q(q) + \omega^Q(q))}{E^2 - [\omega^q(q) + \omega^Q(q) + \Sigma_q + \Sigma_Q]^2}
$$

$$
m(q) = \frac{m_q\, m_Q}{\omega^q(q)\,\omega^Q(q)}.
$$

Riek et al., 2010

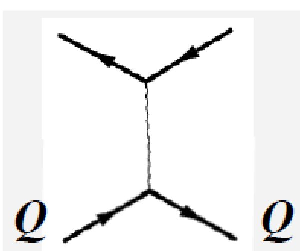

- **momentum transfer**
  $q^2 = q_0^2 - \vec{q}^{\,2} \approx -\vec{q}^{\,2}$
  $q_0 \sim \vec{q}^{\,2}/2m_Q << |\vec{q}|$

➔ static/space-like potential interactions, with relativistic corrections

- **single heavy quark in QGP**
  $p_{\mathrm{th}}^2 \sim 2m_Q T >> T^2$

➔ soft interactions q~T << p_Q

- Soft & (approximately) static Q-Qbar and Q-q/g interactions in QGP
- Common description of heavy quarkonia and single Q transport
- Thermodynamic T-matrix (bound states, scattering states, and resummation)

T-matrix: vacuum constraints

Quarkonia

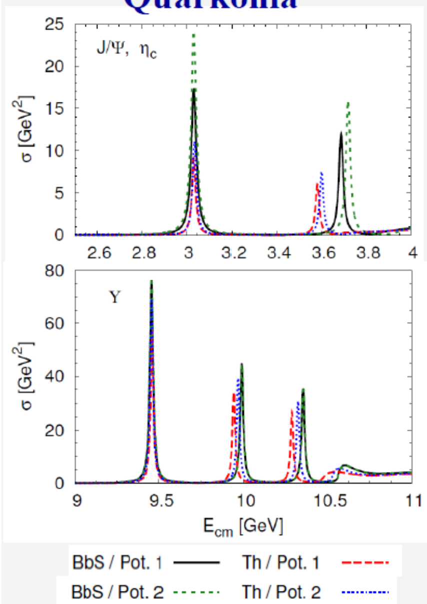

D-Mesons

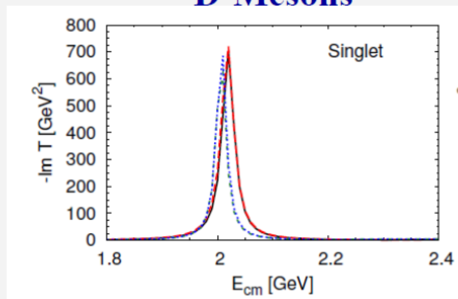

- no hyperfine splitting
- (bare) masses adjusted to ground state
- ~ **±50 MeV** accuracy

		BbS-scheme	Th-scheme
Potential 1	m_c^0	1.355 GeV	1.264 GeV
	m_b^0	4.712 GeV	4.662 GeV
Potential 2	m_c^0	1.402 GeV	1.293 GeV
	m_b^0	4.718 GeV	4.668 GeV

$m_q = 0.4$ GeV, $m_s = 0.55$ GeV

Riek et al., 2010

➔ vacuum spectroscopy well reproduced

➔ Born approximation compared to pQCD

➔ Breit correction essential

$$V_{Q1Q2}(r) \rightarrow V_{Q1Q2}(r)\ (1 - v_1 \cdot v_2)$$

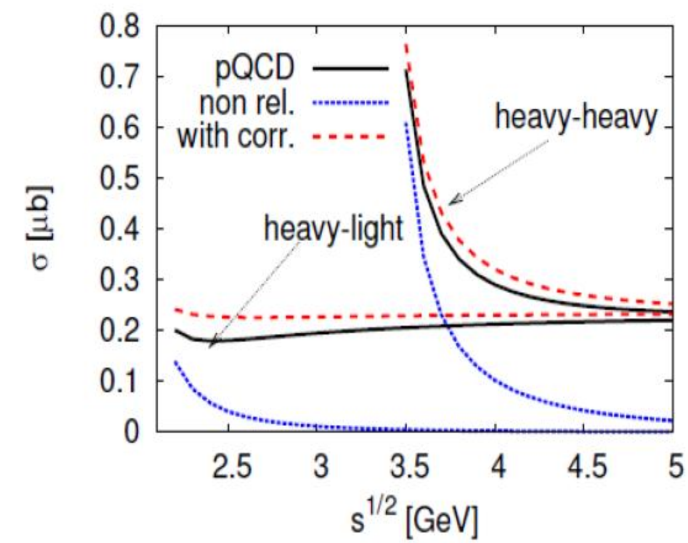

In-medium HQ potential: F or U

$$F_1(r,T) = U_1(r,T) - T\,S_1(r,T)$$

Free Energy

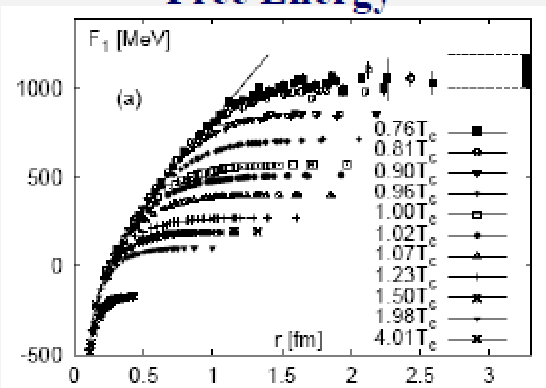

Internal Energy

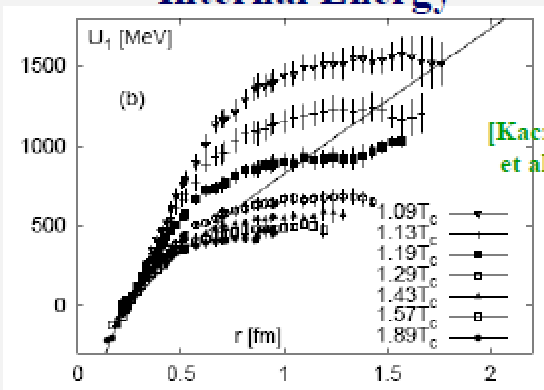

[Kaczmarek et al '05]

- "**weak**" $Q\bar{Q}$ potential
- "**strong**" $Q\bar{Q}$ potential, $U = \langle H_{int} \rangle$

- **F, U, S thermodynamic quantities**
- **Entropy**: many-body effects

(a) Free energy $\mathbf{F_1}$
=> weak $\bar{\mathbf{Q}}\mathbf{Q}$ potential,
small **Q** "selfenergy" $\mathbf{F_1(r=\infty,T)/2}$

(b) Internal Energy $\mathbf{U_1}$ $(U = \langle H_{int} \rangle)$
=> strong $\bar{\mathbf{Q}}\mathbf{Q}$ potential,
large **Q** "selfenergy" $\mathbf{U_1(r=\infty,T)/2}$

- U as proxy for HQ potential is favored by (a) Υ(1S) suppression & (b) charm quark v_2
➔ this will be discussed later

Self-consistent HQ potential: beyond F or U

- For static Q-Qbar in medium: F(Q-Qbar)= F(Q-Qbar + medium) – F(medium)

$$F_{Q\bar{Q}}(T,r) = -T\ln\left(\tilde{Z}_{Q\bar{Q}}\right) = \left(-T\ln\left(Z_{Q\bar{Q}}\right)\right) - \left(-T\ln(Z)\right)$$

$$\tilde{Z}_{Q\bar{Q}} = \frac{Z_{Q\bar{Q}}}{Z} = \frac{{}_n\langle n|\chi(r_2)\psi(r_1)e^{-\beta H}\psi^+(r_1)\chi^+(r_2)|n\rangle}{Z}$$

$$= G^>(-i\tau, r_1, r_2|r_1, r_2)|_{\tau=\beta} = \tilde{G}^>(-i\tau, r\,)|_{\tau=\beta}$$

$$r = r_1 - r_2, \qquad \beta = 1/\mathrm{T}$$

McLerran and Svetitsky, PRD 24 (1981) 450

Blazoit et al., NPA806 (2008) 312–338

$$\boldsymbol{F_{Q\bar{Q}}(T,r) = -T\,ln\left(\tilde{G}^>(-i\tau,r)\right)|_{\tau=\beta}}$$

- Two-particle Green's function: full vs free, z=-iτ: time → energy representation

$$G(z,r) = \frac{1}{[\hat{G}_0(z)]^{-1} - V(z,r)} \qquad \left[G_0^{(2)}\right]^{-1} = z - \Sigma(z)$$

$$\tilde{G}^>(-i\tau,r) = \int_{-\infty}^{\infty} dE\, \frac{-1}{\pi}\mathrm{Im}\left[\frac{1}{\left[\hat{G}_0(E+i\epsilon)\right]^{-1} - V(E+i\epsilon,r)}\right]e^{-\tau E}$$

- Q-Qbar free energy F related to Q-Qbar potential and self-energies

Liu&Rapp, NPA 941 (2015) 179

$$F_{Q\bar{Q}}(r;T) = -T\ln\left[\int_{-\infty}^{\infty}\frac{dE}{\pi}\mathrm{e}^{-\beta E}\mathrm{Im}\left(\frac{-1}{E-\tilde{V}(r;T)-2\Delta m_Q-\Sigma_{Q\bar{Q}}(E,r;T)}\right)\right]$$

→ weakly coupled limit, self-energy Σ→iε →δ(E-V-2m_Q) → V=F
strongly coupled limit, large ImΣ → need a stronger V to match F

Self-consistent HQ potential

- Now heavy-light T-matrix with full spectral functions (off-shell Q, q, g)

$$T^a_{Qi}(E,\mathbf{p},\mathbf{p}') = V^a_{Qi} + \int \frac{d^3k}{(2\pi)^3} V_{Qi}(\mathbf{p},\mathbf{k}) G^0_{Qi}(E,\mathbf{k}) T^a_{Qi}(E,\mathbf{k},\mathbf{p}')$$

$$G^0_{iQ}(E,\mathbf{k}) = \int d\omega_1 d\omega_2 \frac{\rho_i(\omega_1,\mathbf{k})\rho_Q(\omega_2,\mathbf{k})}{E-\omega_1-\omega_2+i\epsilon}[1 \pm f_i(\omega_1) - f_Q(\omega_2)]$$

- Single Q spectral function related with T-matrix again

$$G_Q = 1/[\omega - \omega_Q(k) - \Sigma_Q(\omega,k)] \ , \quad \rho_Q = -\frac{1}{\pi}\mathrm{Im}\ G_Q$$

$$\Sigma_Q(\omega,k) = \int \frac{d^3p_2}{(2\pi)^3} \int d\omega_2 \sum_i \rho_i(\omega_2,p_2) \int \frac{dE}{\pi} \frac{\mathrm{Im}T^{al}_{Qi}(E,\mathbf{k},\mathbf{p_2})}{E-\omega-\omega_2+i\epsilon}[f_i(\omega_2) \mp f(E)]$$

➔ Finally aided with a relation between 2-particle(Q-Qbar) self-energy and 1-particle(Q) self-energy, self-consistent solution of HQ potential and T-matrix with spectral functions /off-shell effects can be performed by fitting the lattice-QCD free energy

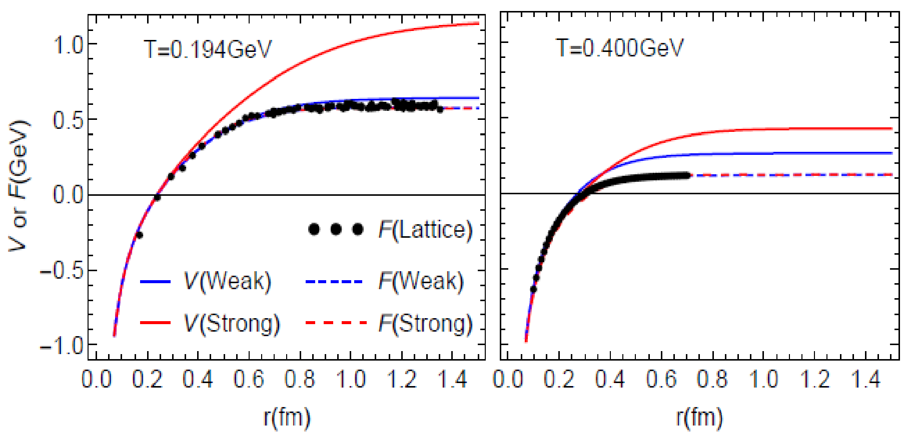

$$V_a(r) = C_a \frac{\alpha_s}{r} e^{-\mu_D T} + \frac{\sigma}{\mu_s}(1 - e^{-\mu_s T})$$

Solutions not unique:
weakly coupled V~ F
VS
Strongly coupled V➔ long range remnant confining Force, not much screening

Liu&Rapp, NPA 941 (2015) 179

Charm-light T-matrix

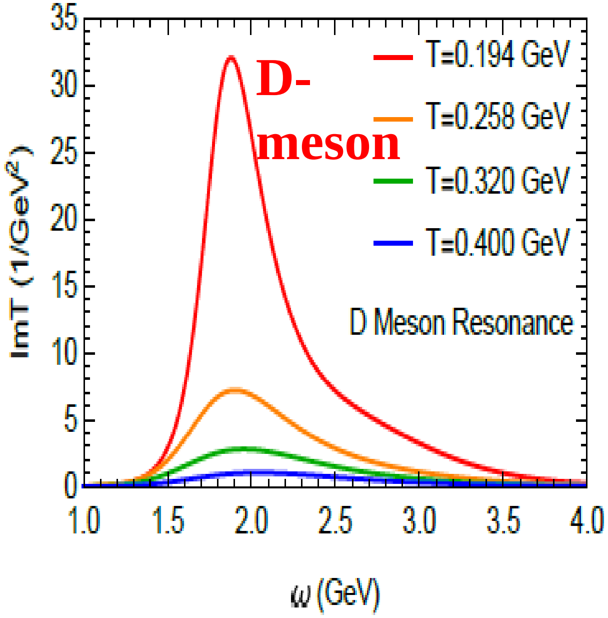

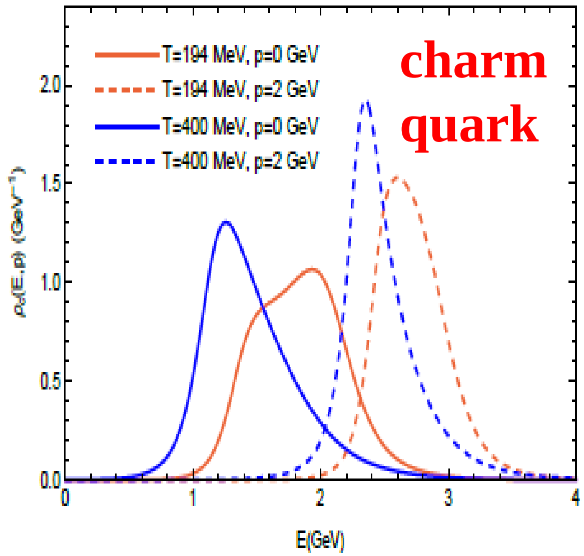

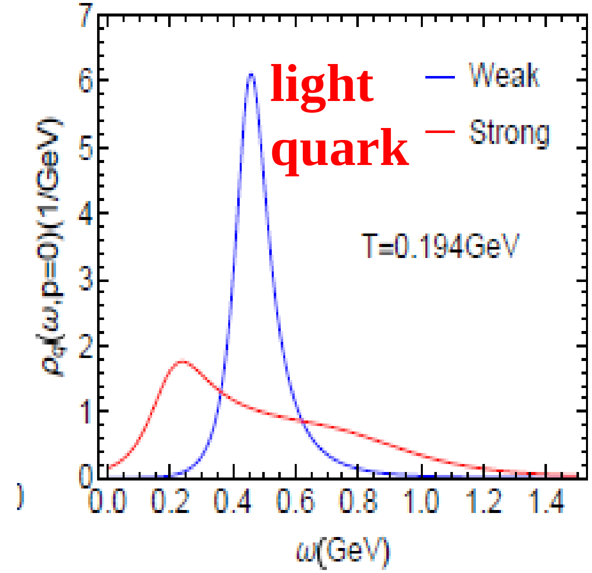

Liu&Rapp, PRC97, 034918 (2018)

- In strongly coupled solution: at low T~194 MeV, light q width~600 MeV > nominal thermal mass ~ 500 MeV ➔ melted, no quasiparticles charm c collisional width similar 500-700 MeV< mass ➔ still good Brownian markers [shoulder in c-spectral due to off-shell scattering with thermal light quarks]

- Charm-light ImT: as T is reduced ➔ V becomes stronger (less screeded) ➔ broad D-meson linear near-threshold resonances ➔ enhancing c-quark thermal relaxation rate [resonances also form in color-antitriplet diquark cq/qq channels]

Charmonia/Bottomonia spectral functions

charmonia **bottomonia**

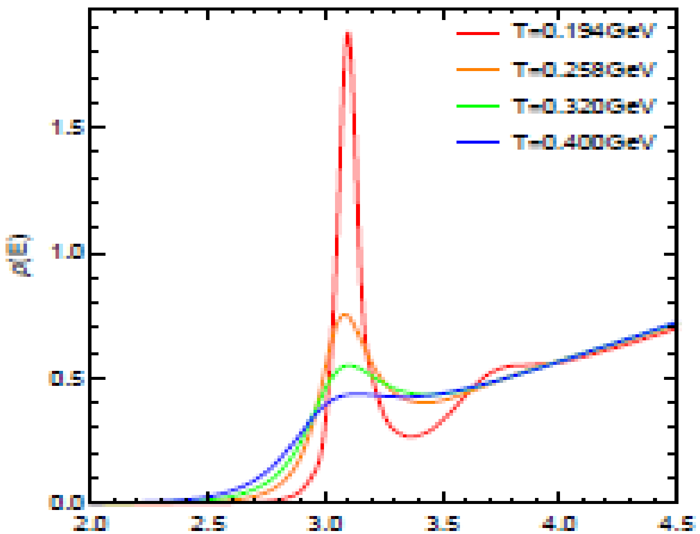

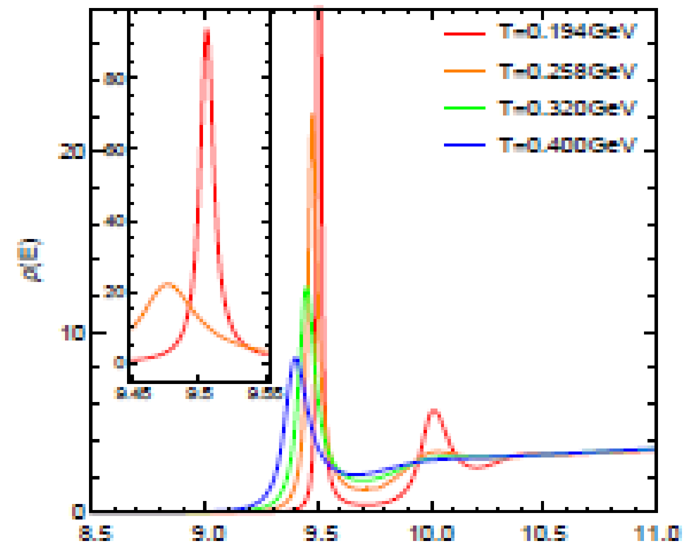

Liu&Rapp, PRC97, 034918 (2018)

Strongly coupled solution with interference effect

- A strong potential V(r,T) ➔ deep bound states for ground states J/ψ, η_c [dissolve at T~300 MeV] and especially for Υ(1S) and η_b [persist for T>400 MeV]
  ➔ their spectral width significantly < $2*\Gamma_c$ or $2*\Gamma_b$ (strong interference effect)
- For excited states ψ(2S), Υ(3S) [dissolves at T~194 MeV] and Υ(2S) [dissolves at T>200 MeV] ➔ their $2*\Gamma_c$ or $2*\Gamma_b$ > $E_{binding}$ thus cannot survive
  spectral width ~ $2*\Gamma_c$ or $2*\Gamma_b$ (interference effect small)

MH et al, 130 (2023) 104020

Heavy quarkonia dissociated not by pure static screening (which is rather weak at T not too far from Tc), but continuously by collisional widths due to single Q width

Constraint from lattice correlator

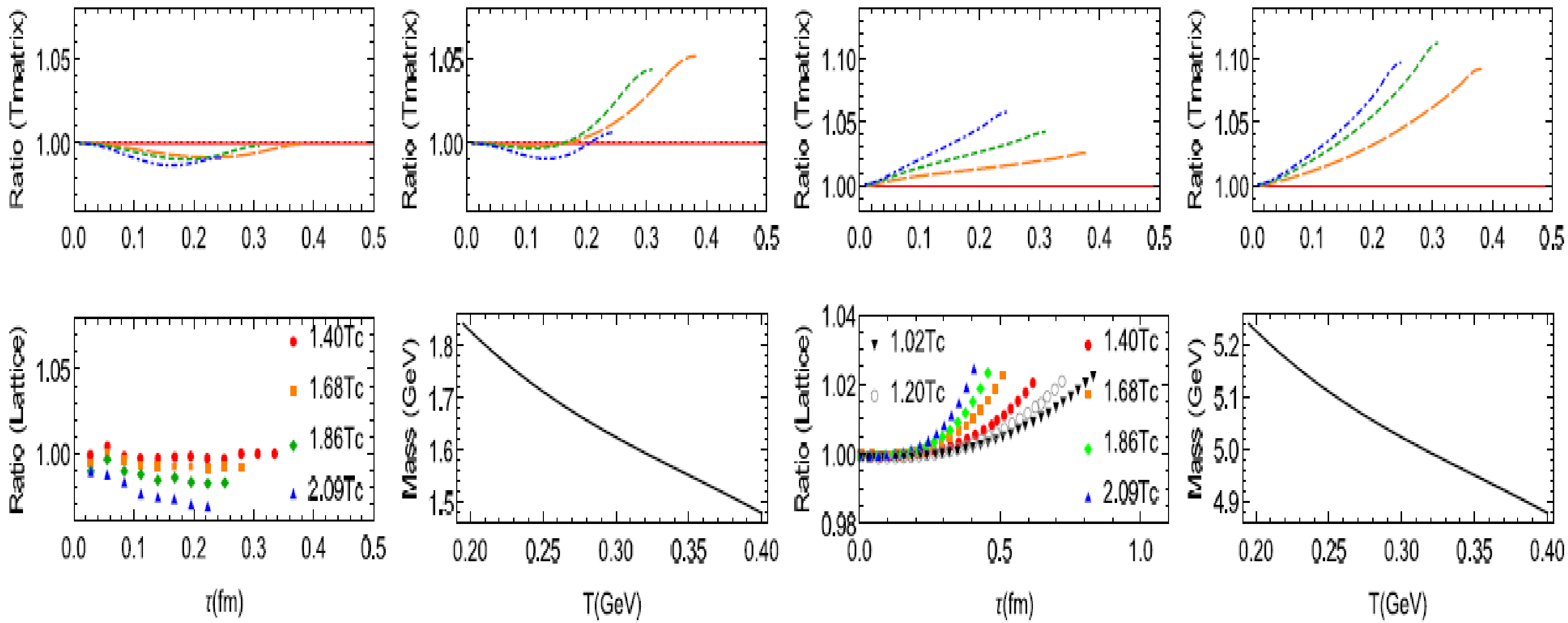

- Euclidean point-to-point correlator accessible to lattice

Liu&Rapp, PRC97, 034918 (2018)

$$G_\alpha(\tau, P; T) = \int d^3 r e^{i\mathbf{P}\cdot\mathbf{r}} \langle j_\alpha(\tau, \mathbf{r}, j_\alpha(0,0)\rangle$$

$$\mathcal{K}(\tau, E; T) = \cosh[E(\tau - 1/2T)]/\sinh[E/2T].$$

$$G_\alpha(\tau; T) = \int_0^\infty dE \rho_\alpha(E, T)\mathcal{K}(\tau, E; T) \qquad R_G^\alpha = \frac{G_\alpha(\tau; T)}{G_\alpha^{\rm rec}(\tau; T)}$$

- Spectral functions with interference effects (1st, 3rd columns) a bit better than without(2nd, 4th), but not decisive ➔ point-split/extended correlators needed to better exhibit spectral modifications **Petreczky et al., PRD100(2019)074506**
- T-dependence of correlator mainly from zero-mode (transport peak), not melting of bound states **Petreczky Eur. Phys. J. C (2009) 62: 85–93**

Charm quark relaxation rate/drag

U vs F vs V(strong vs weak solution) corresponding c-quark thermal relaxation rate

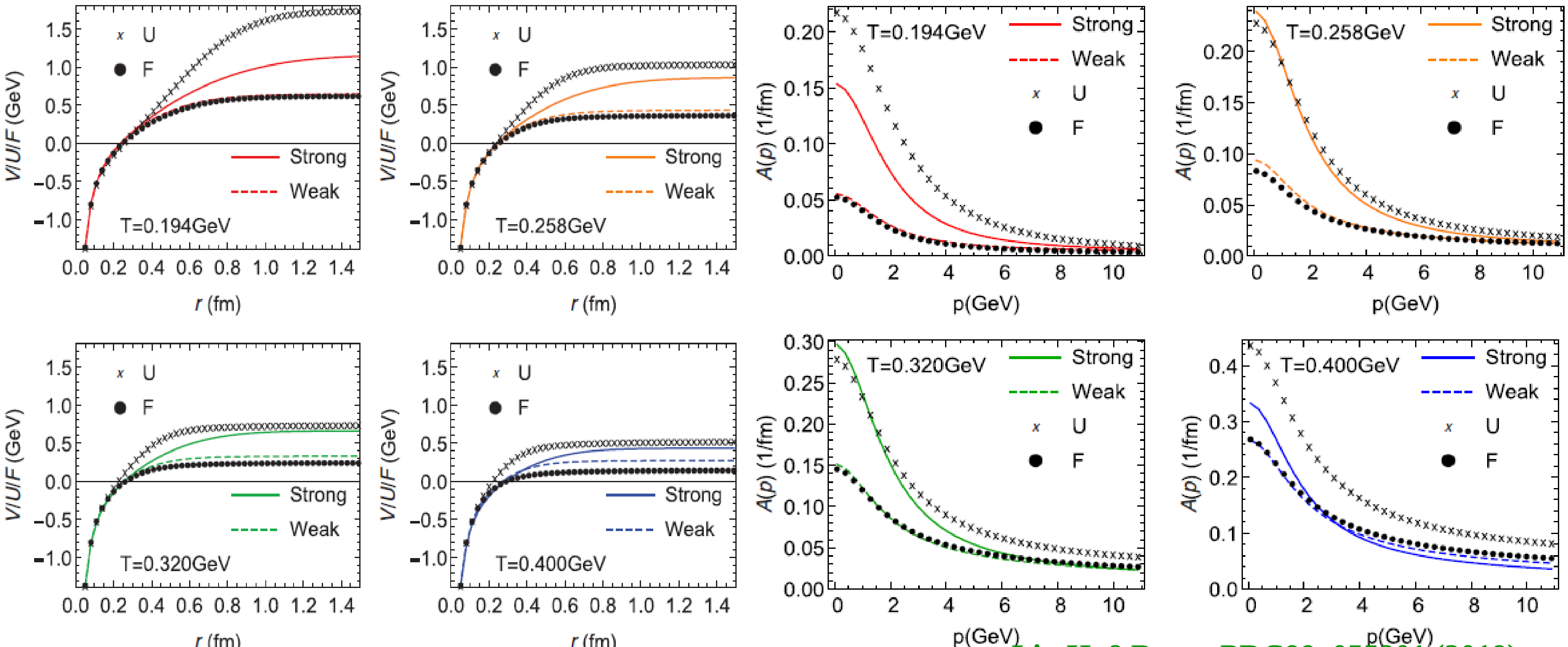

Liu,He&Rapp, PRC99, 055201 (2019)

- F ~ V(weak) ➔ similar A(p,T)
- U & V(strong) ➔ stronger A(p,T) especially at low T and low p [resonant interaction]
- V(strong) features long-range remnant confining force (-dV/dr) to encompass more near-by thermal partons ➔ instrumental for large A(p=0)!

Charm quark A(p=0,T)

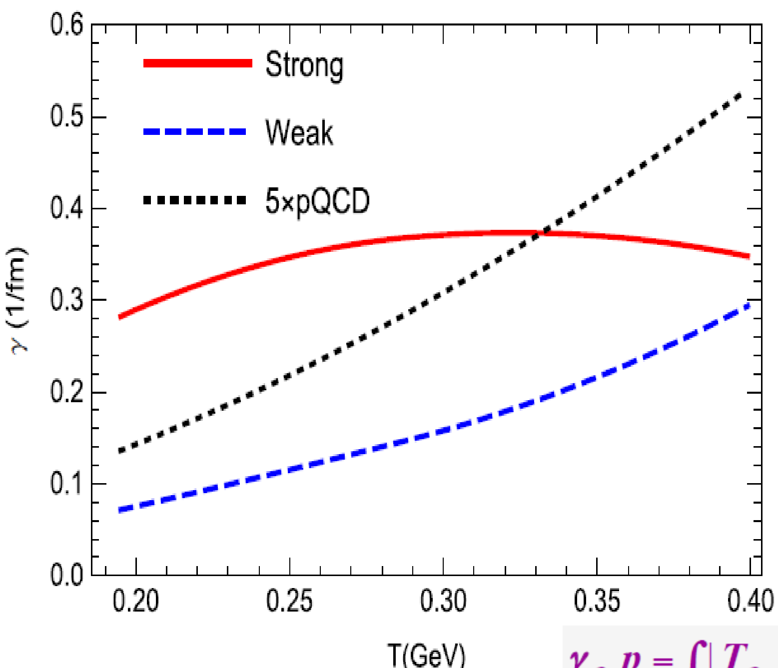

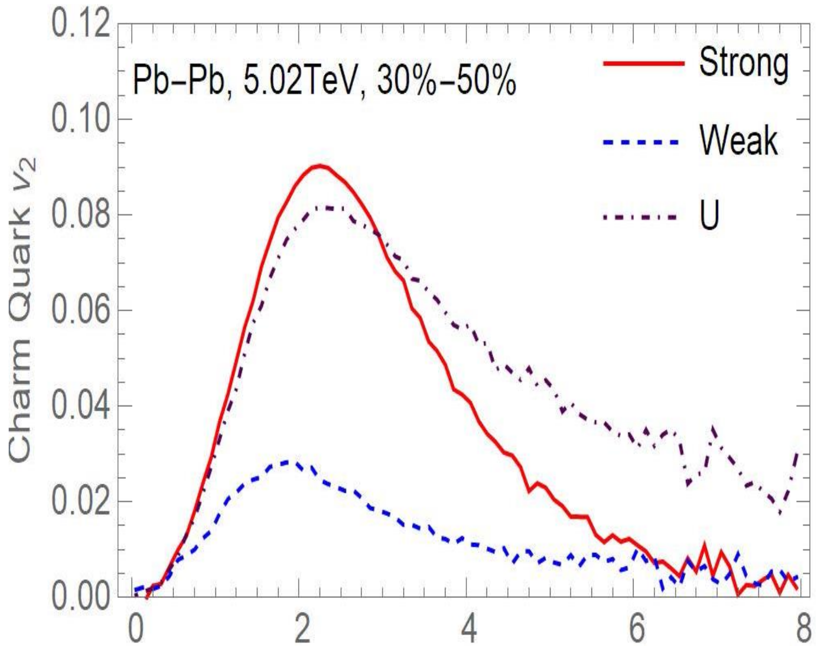

$$\gamma_Q\, p = \int |T_{Qq}|^2 (1-\cos\theta)\ f^{q,g}$$

- γ=A(p=0,T) ~ 0.3/fm from strongly coupled solution ➔ thermal relaxation time τ ~ 3 fm/c for very low p charm quarks (p-dependence converging to pQCD at high p)
- 5*LO-pQCD is still not enough; weakly coupled interaction also far off
- Strongly coupled solution γ rather stable vs T: resonant enhancement at low T
- Charm quark v_2 at p_T~ 2 GeV: sensitive measure of charm coupling strength

Liu,MH&Rapp, PRC99, 055201 (2019)

Landscape of T-matrix HQ & quarkonium interactions

Remnant confining force

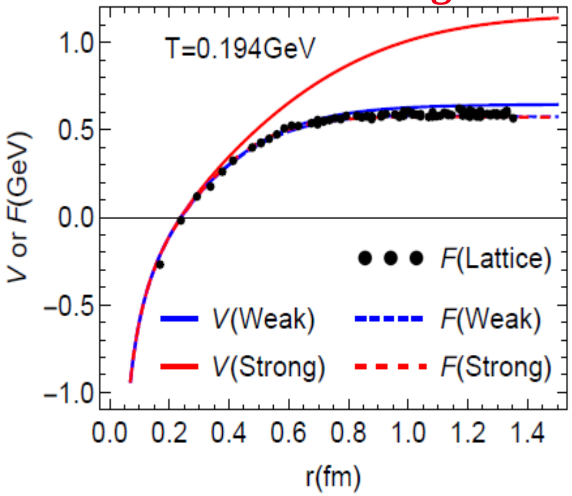

Resonances form near T_c

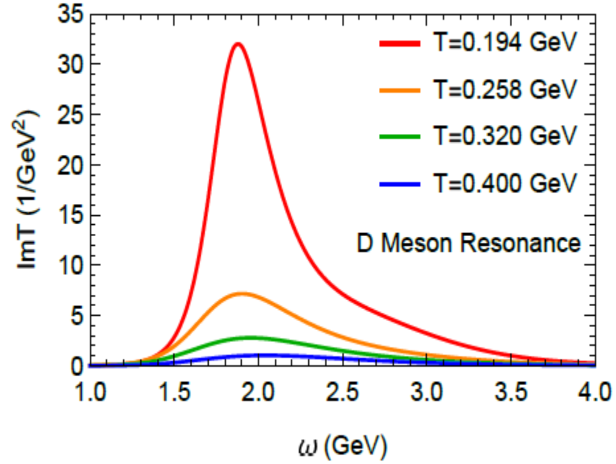

Accelerates thermalization

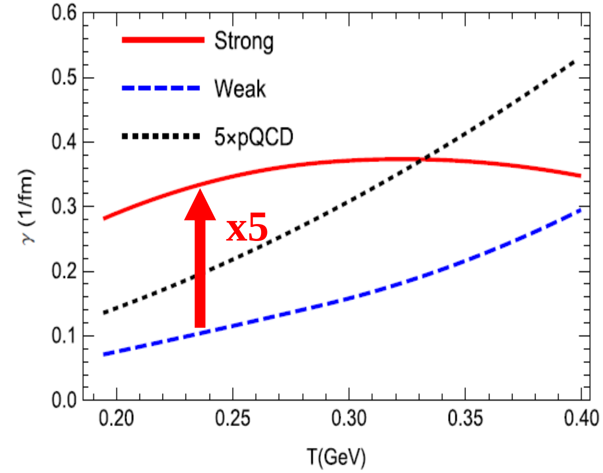

J/ψ survives in QGP

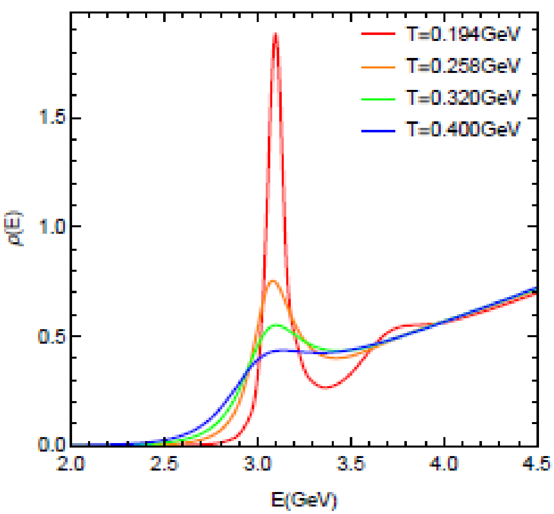

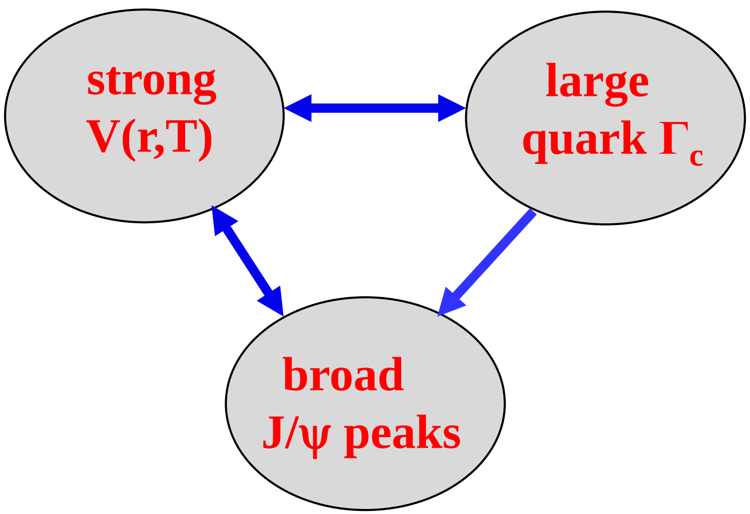

Coupling strength ↔ HQ v_2

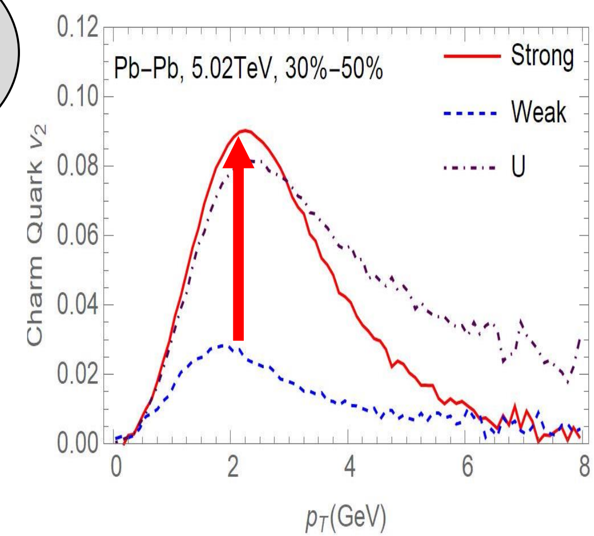

Comparison of A(p,T) in different models

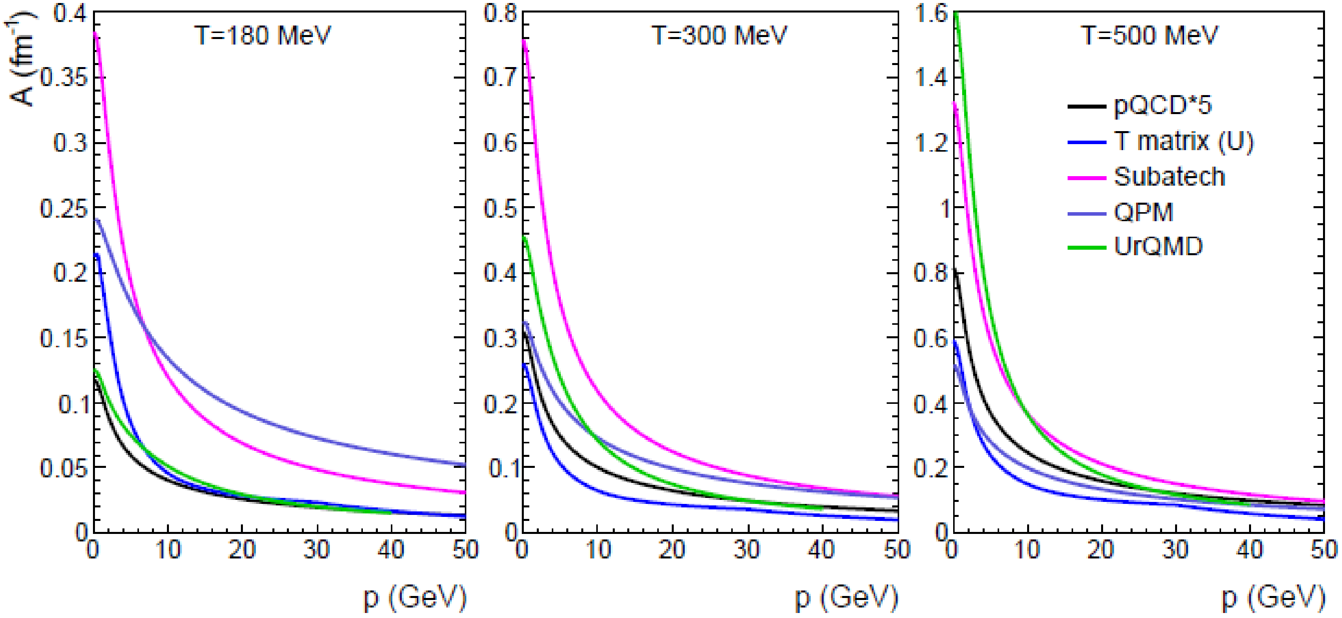

Figure 3.1: Friction coefficients for charm-quark diffusion in the QGP as a function of three-momentum for three different temperatures from various model calculations: black lines: pQCD Born diagrams with α_s=0.4, multiplied with and overall K-factor of 5, blue lines: T-matrix results using the internal-energy (U) as potential proxy [20, 89], pink lines: pQCD with running coupling constant and reduced Debye mass [24, 25], purple lines: quasiparticle model with coupling constant fitted to the lQCD EOS [63], and green lines: D-meson resonance model [26]; figure taken from Ref. [61].

- Subatech/Nantes (Born diagram with running coupling and reduced m_D) largest at low p – driven by large coupling strength for soft momentum transfers
- T-matrix with U-potential smaller at low p, and drop-off vs p due to transition from a resumed string force at large distance to color-Coulomb force at small distances
- QPM(Catania) comparable to T-matrix at low p, but much flatter toward high p > Nates at T~180 MeV

Lattice-QCD HQ diffusion

- Vector meson spectral function encoding a transport peak

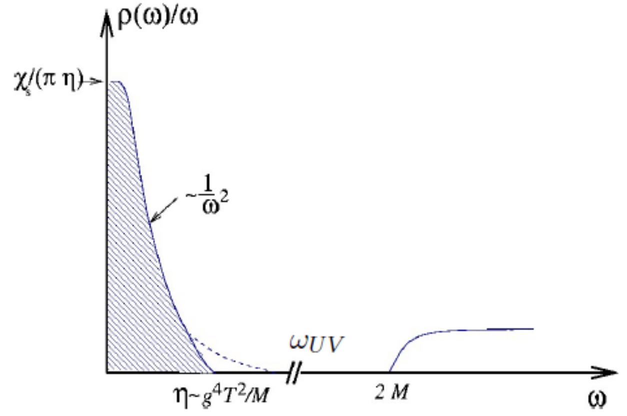

$$\rho_V^{\mu\nu}(\omega) \equiv \int_{-\infty}^{\infty} \mathrm{d}t e^{i\omega t} \int \mathrm{d}^3x \left\langle [\hat{J}^\mu(t,\vec{x}), \hat{J}^\nu(0,\vec{0})] \right\rangle$$

$$\sum_i \frac{\rho_V^{ii}(\omega)}{\omega} \simeq 3\chi_2^q \frac{T}{M}\frac{\eta}{\eta^2+\omega^2}, \quad \omega < \omega_{UV}, \quad \eta = \frac{T}{M}\frac{1}{D}$$

Petreczky, Teaney, PRD 72 ('06) 014508

drag constant

- HQ drag coefficient ~ width of the peak in the limit ω→0

$$\kappa = 2\,MT\eta = 2\,T^2/Ds$$

For large quark mass the transport peak is very narrow even for strong coupling and its difficult to reconstruct it accurately from Euclidean correlator calculated on the lattice

TABLE V. Estimated ranges for η/T using the thermal ratio $R^{2,0}$ and resultant $2\pi TD$ with a mass of $M_c = 1.28$ GeV and $M_b = 4.18$ GeV. For some temperatures, the method did not work out to yield a result.

	Charm		Bottom	
T/T_c	η/T	$2\pi TD$	η/T	$2\pi TD$
1.1	–	–	–	–
1.3	<0.27	>7.48	–	–
1.5	0.85–2.78	0.84–2.73	–	–
2.25	3.32–5.28	0.66–1.05	0.29–1.10	0.97–3.66

Ding et al., PRD104, 114508 (2022)

- Using mid-point correlator (τT=0.5) and a model spectral function, Ding et al. extracted a larger drag for charm than bottom at T=2.25Tc $\rho_{ii}^{\mathrm{mod}}(\omega) = A\rho_V^{\mathrm{pert}}(\omega - B)$

- In the heavy quark limit, Ds=T/mγ independent of heavy quark mass

Lattice-QCD HQ diffusion

- In the heavy quark limit (quenched approximation) ➔ chromo-electric field correlators

$$G_E(\tau) = -\frac{1}{3}\sum_{i=1}^{3} \frac{\left\langle \mathrm{ReTr}\left[U(\beta,\tau)\, gE_i(\tau,\vec{0})\, U(\tau,0)\, gE_i(0,\vec{0})\right]\right\rangle}{\left\langle \mathrm{ReTr}[U(\beta,0)]\right\rangle}$$

Transport coefficient ~ intercept of the spectral function not its width

$$\kappa = \lim_{\omega\to 0} \frac{2T}{\omega}\rho_E(\omega)$$

$$G_E(\tau) = \int_0^\infty \frac{d\omega}{\pi}\rho_E(\omega)\frac{\cosh\left(\tau - \frac{1}{2T}\right)\omega}{\sinh\frac{\omega}{2T}}$$

Caron-Huot, Laine, Moore, JHEP 0904 ('09) 053

Francis, Kaczmarek, Laine, et al, PRD 92 ('15) 116003

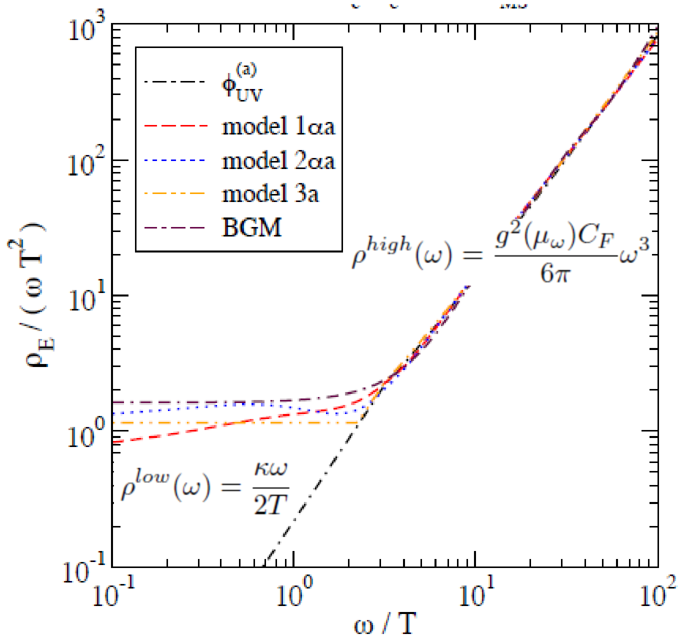

- Can lattice go to finite momentum ?

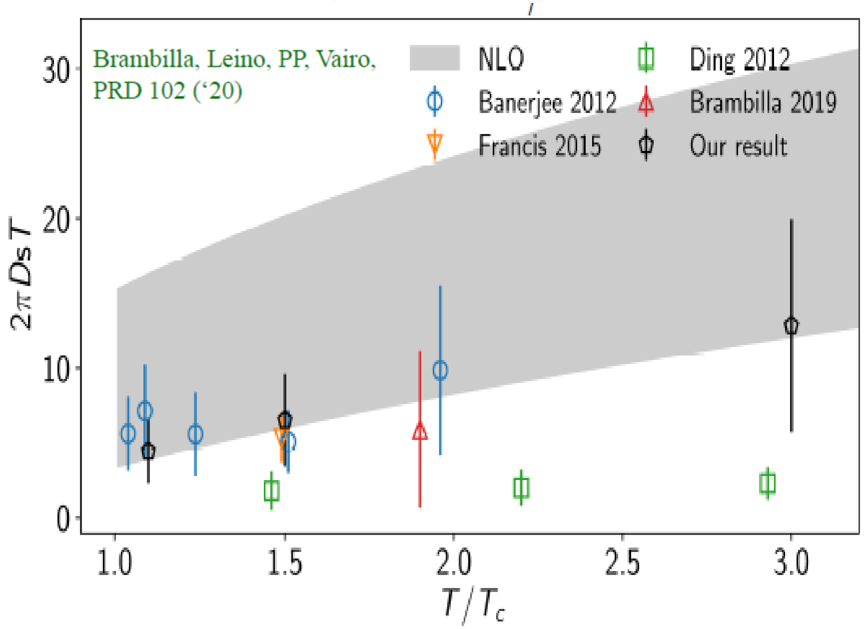

Lattice-QCD HQ diffusion -- latest

- In the heavy quark limit (unquenched, full QCD) chromo-electric field correlator

$$G_E = -\sum_{i=1}^{3} \frac{\langle \mathrm{ReTr}[U(1/T,\tau)E_i(\tau,\mathbf{0})U(\tau,0)E_i(0,\mathbf{0})]\rangle}{3\langle \mathrm{ReTr}U(1/T,0)\rangle}. \qquad G_E(\tau,T) = \int_0^\infty \frac{d\omega}{\pi}\rho_E(\omega,T)\frac{\cosh[\omega\tau - \omega/(2T))]}{\sinh[\omega/(2T)]}$$

- Spectral function → HQ diffusion coefficient $\kappa(T) = 2T\lim_{\omega\to 0}[\rho_E(\omega,T)/\omega]$
  ➔ model spectral function: small vs high energy

$$\rho_E(\omega,T) \simeq \rho_{\mathrm{IR}}(\omega,T) = \kappa\omega/(2T) \qquad \rho_E(\omega \gg T) = \rho_{\mathrm{UV}}(\omega) = K\rho_{\mathrm{LO,NLO}}(\omega)$$

Kaczmarek et al., PRL130, 231902 (2023)

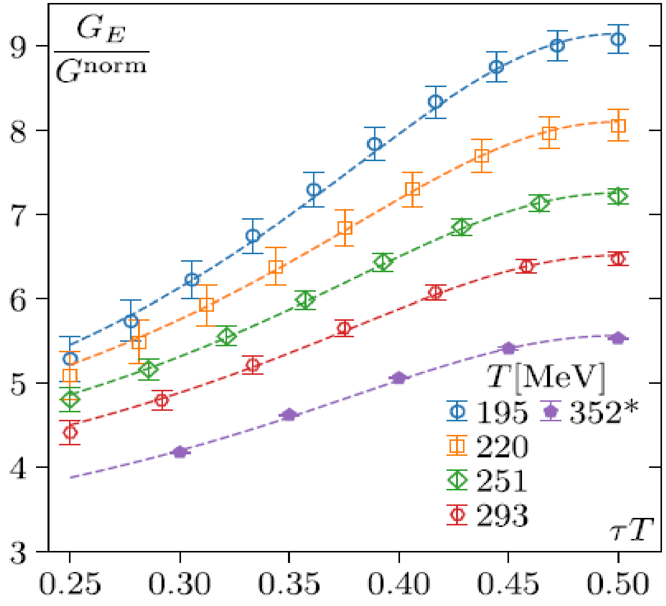

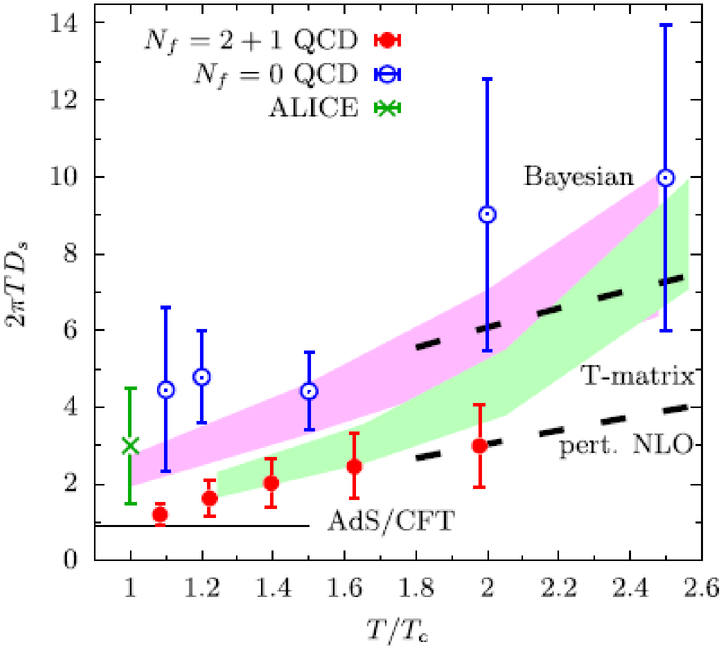

D-meson diffusion in HRG

- D mesons diffusing in HRG, via interactions with light hadrons

Tolos et al., PRC90, 054909(2014)

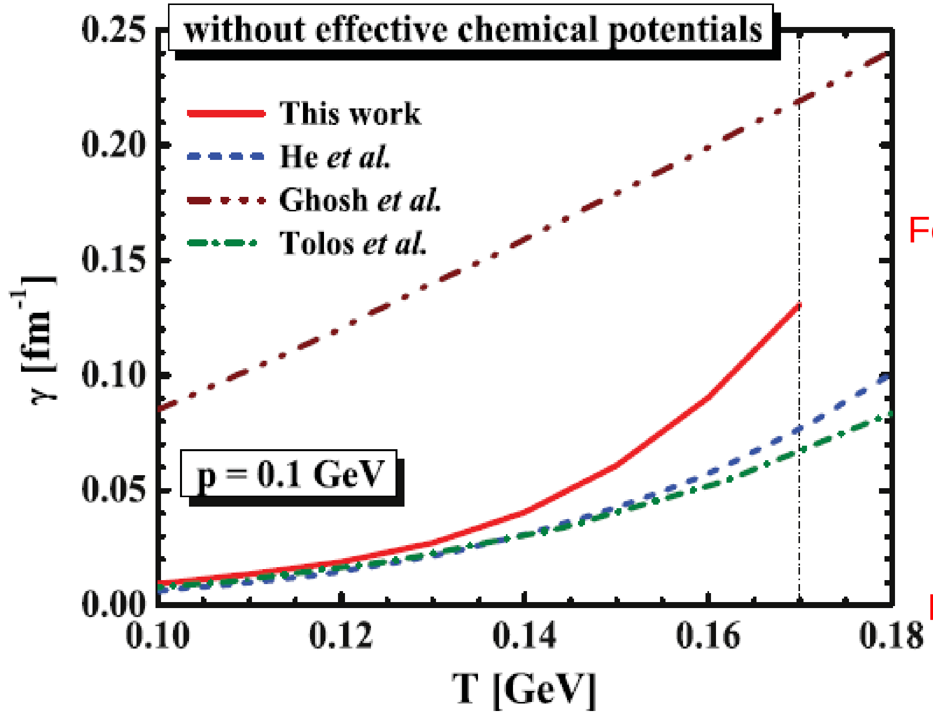

Figure 3. Thermal relaxation rate of low-momentum D mesons in hadronic matter in chemical equilibrium, computed in the approaches of [98] (dashed line), [99] (dash-double-dotted line), [101] (dash-dotted line) and [102] (solid line). Figure taken from [102].

$$A(p,T) = \frac{\gamma_h}{2E_D}\int \frac{1}{(2\pi)^9}\frac{d^3q}{2E_h}\frac{d^3p'}{2E'_D}\frac{d^3q'}{2E'_h} f^h(E_h;T) \times \overline{|\mathcal{M}_{Dh}|^2}(2\pi)^4\delta^{(4)}(p+q-p'-q')\left(1-\frac{\vec{p}\cdot\vec{p}\,'}{\vec{p}^2}\right) \equiv \left\langle\!\!\left\langle 1-\frac{\vec{p}\cdot\vec{p}\,'}{\vec{p}^2}\right\rangle\!\!\right\rangle$$

For a pion gas (dominates at low T~100 MeV):

- Laine (2011) heavy-meson ChPT➔ γ_D~0.05/fm
  Ghosh(2011) Born diagrams ➔ γ_D~0.08/fm
- He,Fries,Rapp(2011) empirical scattering amplitudes (resonance) ➔ γ_D~0.005/fm
- Tolos et al.(2011) Unitarized ChPT ➔resonance ➔ γ_D~0.08/fm

For full HRG:

- Substantial contributions from higher states as temperature tends to Tc from below

D-meson diffusion in HRG

- D + light hadron empirical scattering amplitudes/cross sections

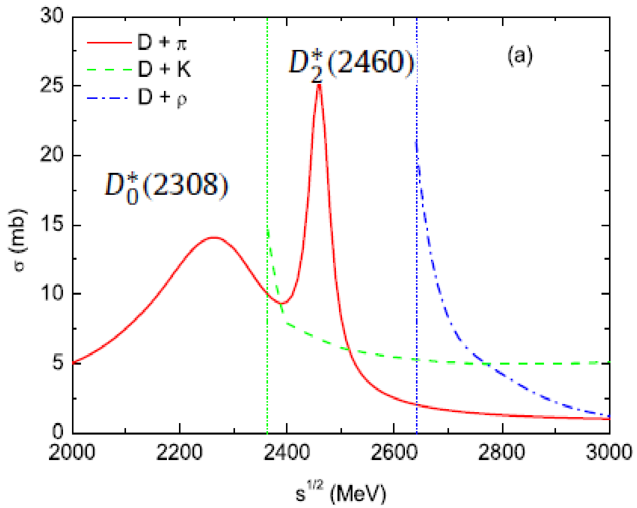

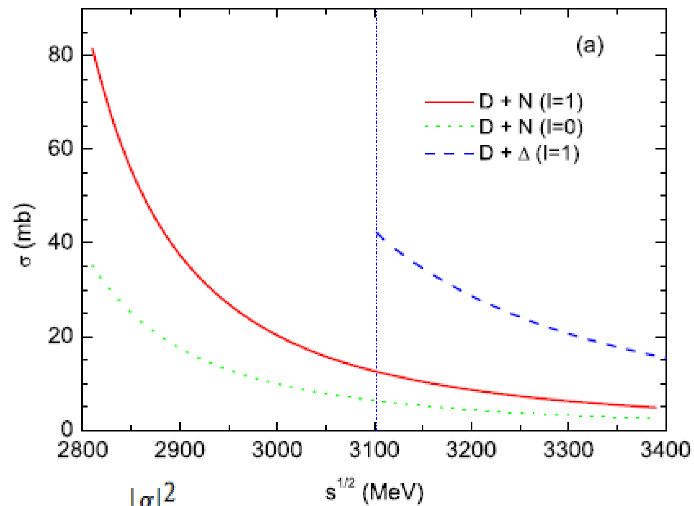

$$\mathcal{M}(s,\Theta=0)=\sum_{j=0}^{2}\frac{8\pi\sqrt{s}}{k}\frac{(2j+1)\sqrt{s}\Gamma_j^{D\pi}}{s-M_j^2+i\sqrt{s}\Gamma_j^{tot}}$$

$$T(\sqrt{s})=\frac{|g|^2}{\sqrt{s}-m_R+i\Gamma_R/2}$$

- Contributions to γ_D from different light mesons/baryons; well approximated by light constituent q-q scattering with σ=3-4 mb

- At high T~Tc, baryon excitations important

He,Fries,Rapp, PLB701(2011)445

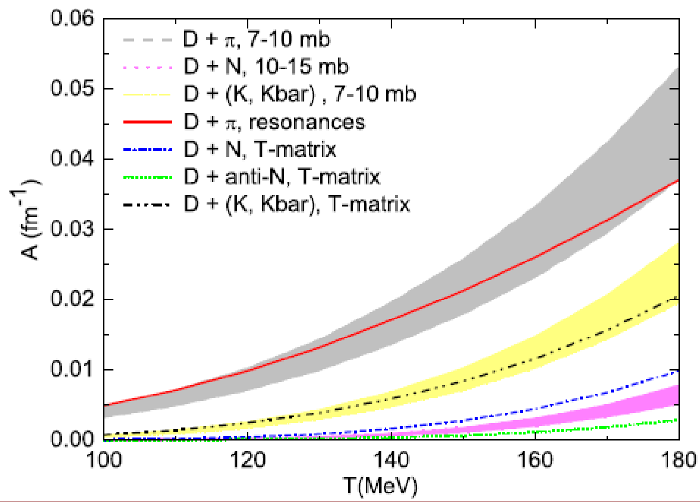

D-meson diffusion in HRG

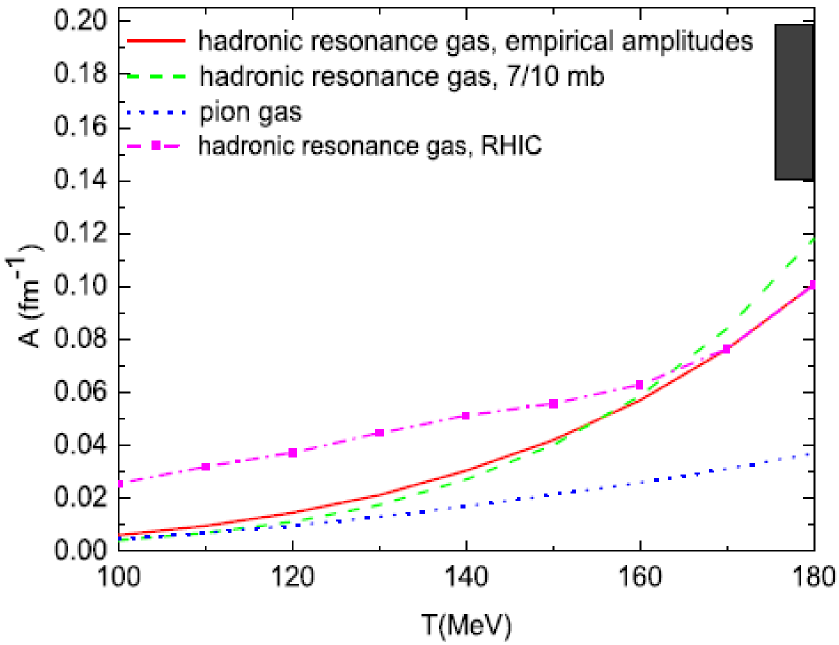

Contributions to the thermal D-meson thermal relaxation rate at $T = 180$ MeV indicating the quantum numbers of the included scattering channels with L: partial wave, I: isospin and J: total angular momentum.

Hadrons	$L_{I,2J}$	A [fm^{-1}]
π	$S_{1/2,0}$, $P_{1/2,2}$, $D_{1/2,4}$, $S_{3/2,0}$	0.0371
$K+\eta$	$S_{0,0}$, $S_{1,0}$	0.0236
$\rho+\omega+K^*$	$S_{1/2,2}$, $S_{0,2}$, $S_{1,2}$	0.0129
$N+\bar{N}$	$S_{0,1}$, $S_{1,1}$	0.0128
$\Delta+\bar{\Delta}$	$S_{1,3}$	0.0144

- D-meson thermal relaxation rate at low momentum near Tc ~0.1 /fm ➔ relaxation time ~ 10 fm/c, already comparable to the fireball lifetime

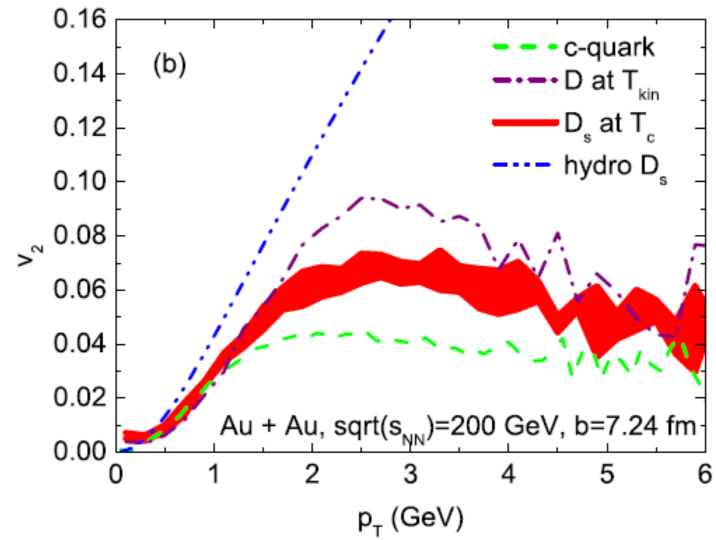

- Enhancing the D-meson v_2 by 20-30% at intermediate p_T, because the background bulk v_2 already almost fully built up by Tc

MH, Fries, Rapp, PRL110, 112301 (2013)

Summary: transport coefficient: $\mathcal{D}_s(2\pi T)$

❖ HQ spatial diffusion coefficient: $\mathcal{D}_s = T/m_Q A(p=0) = T/m_Q \gamma$

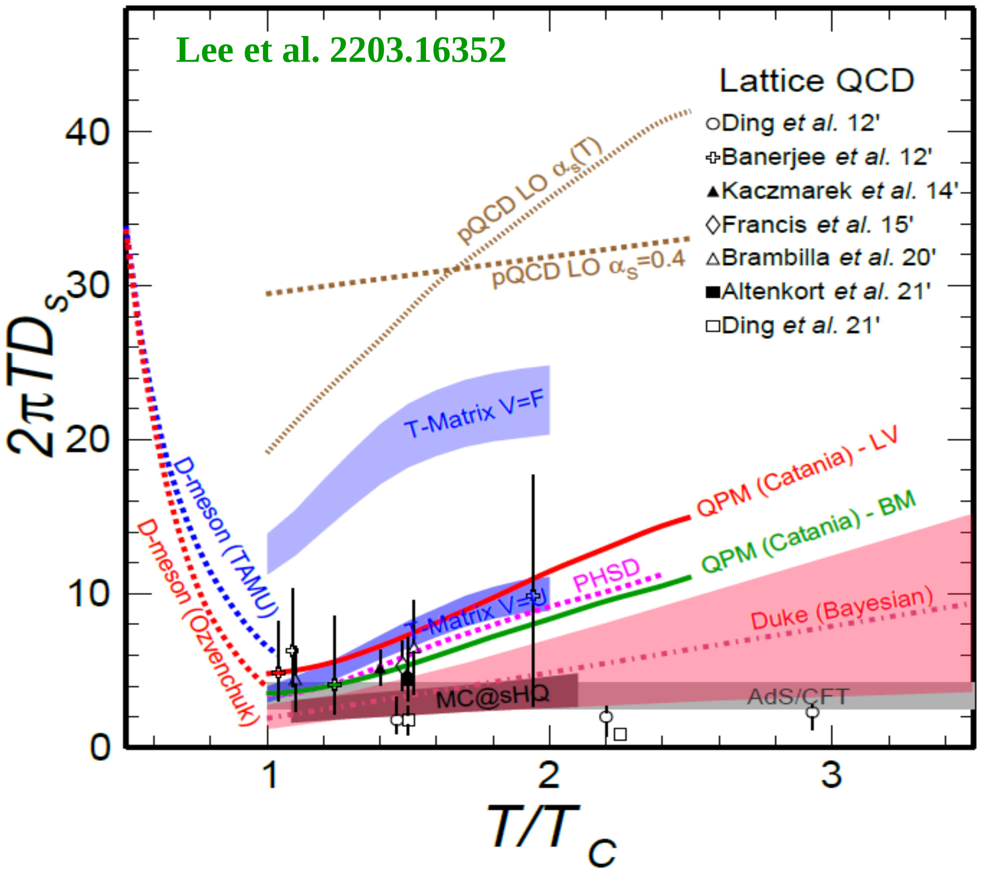

- models & lattice $\mathcal{D}_s(2\pi T)$~2-4 near T_c, x10 smaller than pQCD, scattering rate Γ_{coll} ~3/$\mathcal{D}_s$ ~1 GeV > $M_{q,g}$ ➔ thermal partons melt, Brownian markers survive

- maximum coupling strength near T_c, remnant of confining force?!

- minimum structure across T_c, analogous to η/s

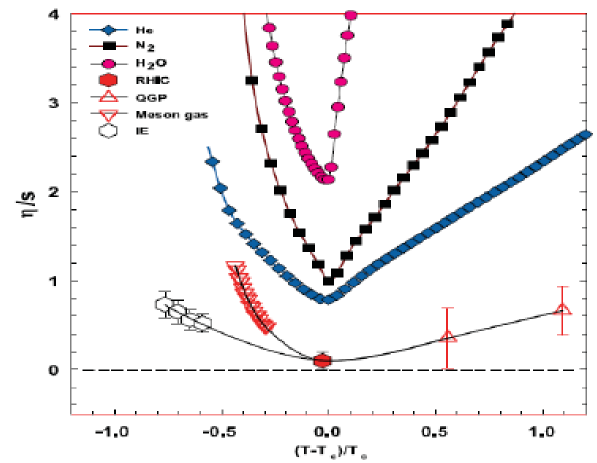

HQ radiative e-loss

- elastic collisions VS medium-induced gluon radiation

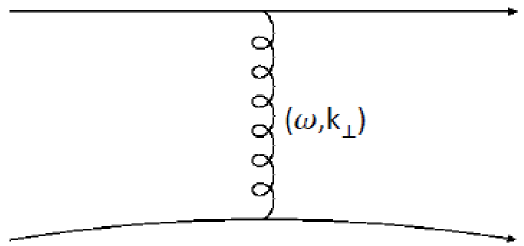

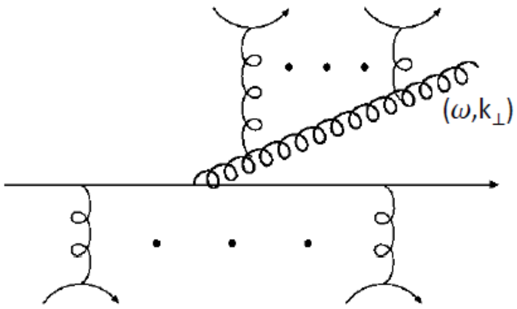

- Factorized elastic * radiation probability

Gossiaux et al., PRD 89 074018 (2014)

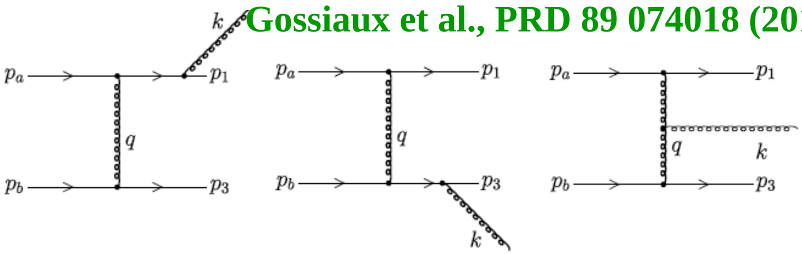

$$\frac{\omega d^4\sigma^{rad}}{dx d^2k_t dq_t^2} = \frac{N_c\alpha_s}{\pi^2}(1-x)\cdot\frac{d\sigma^{el}}{dq_t^2}\cdot P_{rad}$$

k_t , ω = transv mom/ energy of gluon E = energy of the heavy quark

$$P_{rad} = C_A\left(\frac{\vec{k}_t}{k_t^2+(\omega/E)^2m^2} - \frac{\vec{k}_t-\vec{q}_t}{(\vec{q}_t-\vec{k}_t)^2+(\omega/E)^2m^2}\right)^2$$

Emission from heavy q

Emission from g

LPM effect

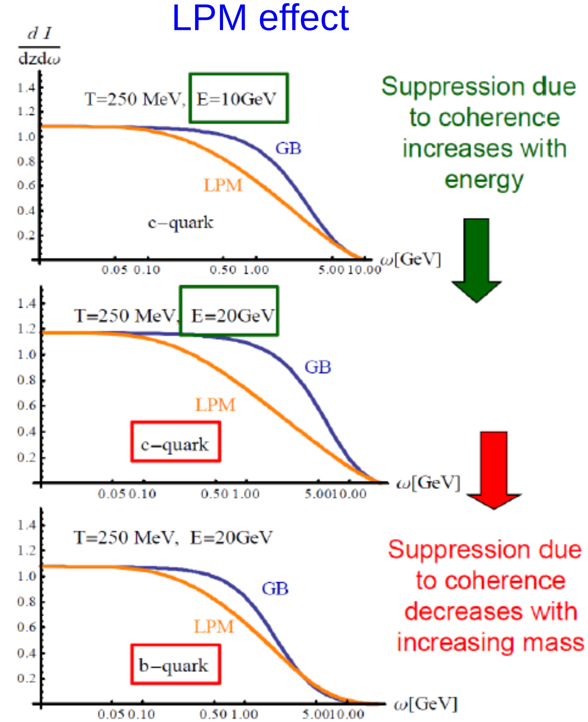

HQ radiative e-loss

- Higher Twist formalism

$$\frac{dN_g}{dx dk_\perp^2 dt} = \frac{2\alpha_s C_A P(x)}{\pi k_\perp^4}\hat{q}\left(\frac{k_\perp^2}{k_\perp^2 + x^2M^2}\right)^4 \sin^2\left(\frac{t-t_i}{2\tau_f}\right)$$

$$\tau_f = 2Ex(1-x)/(k_\perp^2 + x^2M^2)$$

Zhang, Wang, and Wang, PRL93, 072301 (2004)

- Average number of radiated gluons & probability of radiation within △t

$$\langle N_g\rangle(t,\Delta t) = \Gamma_{\text{inel}}\Delta t = \Delta t \int dx dk_\perp^2 \frac{dN_g}{dx dk_\perp^2 dt}$$

$$P_{inel} = 1 - e^{-\langle N_g\rangle}$$

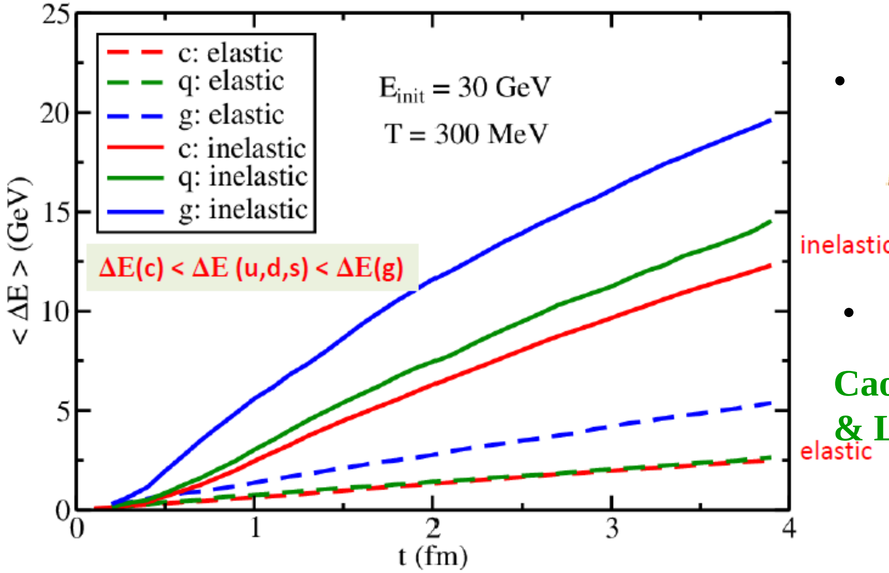

- Implemented in LBT

$$p_1 \cdot \partial f_1(x_1, p_1) = E_1(C_{\text{el}} + C_{\text{inel}})$$

- Flavor hierarchy of e-loss quantified

Cao, Qin and Bass, PLB777(2018) 255
& Liu et al, Eur. Phys. J. C (2022) 82:350

HQ hadronization (I): SHMc

- Statistical hadronization model (SHM) for light quarks:

grand-canonical partition function for HRG

$$\ln Z_i = \frac{V g_i}{2\pi^2} \int_0^\infty \pm p^2 \mathrm{d}p \ln[1 \pm \exp(-(E_i - \mu_i)/T)]$$

$$T_{CF} = 156.6 \pm 1.7 \ \mathrm{MeV}$$

$$\mu_B = 0.7 \pm 3.8 \ \mathrm{MeV} \quad V = 4175 \pm 380 \ \mathrm{fm}^3$$

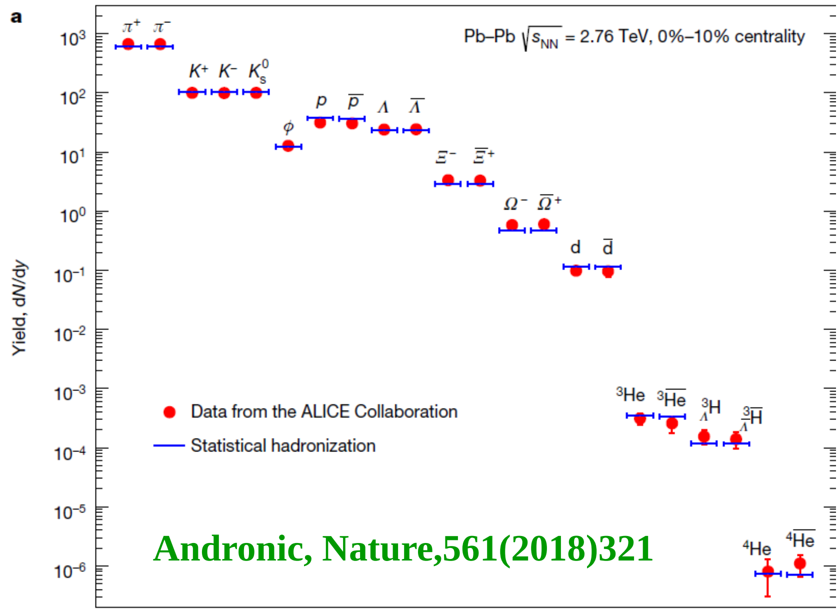

- Statistical hadronization model for charm quarks (SHMc) :
  - charm balance equation $N_{c\bar{c}} = \frac{1}{2} g_c V \sum_{h^i_{oc,1}} n_i^{\mathrm{th}} + g_c^2 V \sum_{h^j_{hc}} n_j^{\mathrm{th}} + \frac{1}{2} g_c^2 V \sum_{h^k_{oc,2}} n_k^{\mathrm{th}}$

where $N_{c\bar{c}} \equiv \mathrm{d}N_{c\bar{c}}/\mathrm{d}y$ = T_{AA}*$d\sigma^{ccbar}$/dy is the charm quark number per unit rapidity,

- thermalized c-quarks hadronized at T_c (strict charm conservation➔ canonical correction)

$$\frac{\mathrm{d}N(h^i_{oc,\alpha})}{\mathrm{d}y} = g_c^\alpha \, V \, n_i^{\mathrm{th}} \frac{I_\alpha(N_c^{\mathrm{tot}})}{I_0(N_c^{\mathrm{tot}})} \quad \propto g_c^\alpha \leftarrow d\sigma^{cc}/dy$$

- p_T-spectrum modelled by hydrodynamic blast wave at T_c

Hadronization: SHMc Andronic, et al., JHEP07(2021)035

- SHMc: open-charm statistical hadronization at T_c $\frac{dN(h^i_{oc,\alpha})}{dy} = g_c^\alpha\, V\, n_i^{th} \frac{I_\alpha(N_c^{tot})}{I_0(N_c^{tot})}$
  - multicharm baryons α=1,2,3 emerging pattern
  - yields enhanced by $g_c^\alpha \sim 30^\alpha$ than pure thermal →strong signal of deconfinement

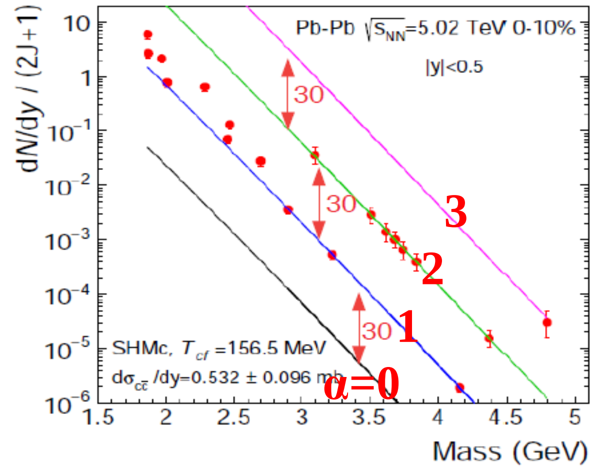

- SHMc yields + blast wave→p_T spectra

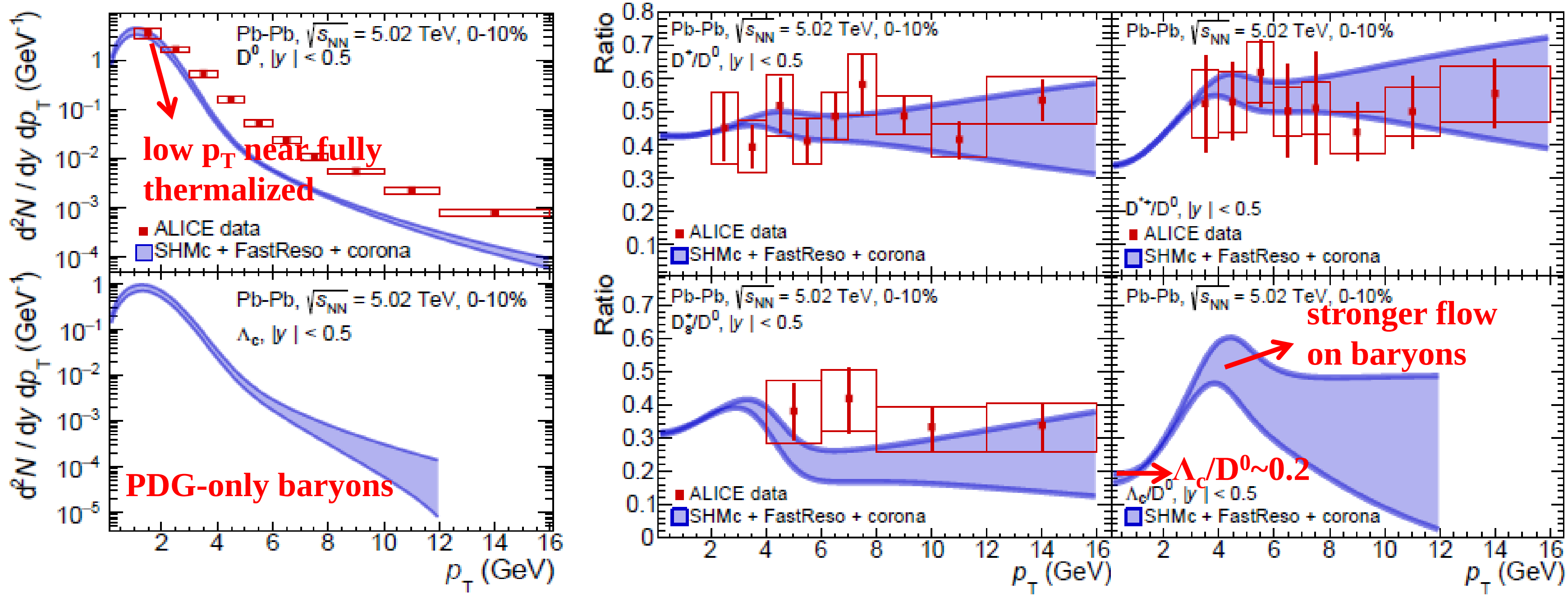

HQ hadronization (II): coalescence

Coalescence: 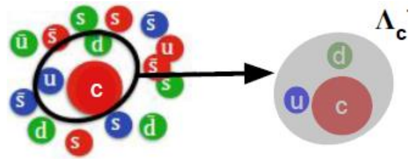

vs. Fragmentation 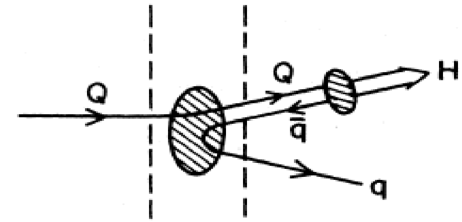

- recombination of low p_T HQs with thermal light quarks nearby in (x&p) phase space ➔ add momentum & flow to the parent HQ
- HQ independent fragmentation into HF hadrons ➔ dominant at high p_T

❖ Instantaneous coalescence models (ICM)

Fries et al., Greco et al., Voloshin '03

$$\frac{d^2N_H}{dP_T^2} = g_H \int \prod_{i=1}^{n} \frac{d^3p_i}{(2\pi)^3E_i} p_i \cdot d\sigma_i \; f_{q_i}(x_i,p_i) \times f_H(x_1..x_n,p_1..p_n)\,\delta^{(2)}\left(P_T - \sum_{i=1}^{n} p_{T,i}\right)$$

- Instantaneous projection via Wigner function

$$f_M(x_1,x_2;p_1,p_2) = \frac{9\pi}{2}\,\Theta\left(\Delta_x^2 - x_r^2\right) \times \Theta\left(\Delta_p^2 - p_r^2 + \Delta m_{12}^2\right)$$

$$f_B = \frac{81\pi^2}{4}\Theta\left(\Delta_x^2 - \frac{1}{2}x_{r1}^2\right) \times \Theta\left(\Delta_p^2 - \frac{1}{2}p_{r1}^2\right) \Theta\left(\Delta_x^2 - x_{r2}^2\right) \times \Theta\left(\Delta_p^2 - p_{r2}^2 - \Delta m_{123}^2\right),$$

- Heinsenberg's uncertaity principle: $\Delta_x \cdot \Delta_p \approx 1$
- successful in explaining B/M, v_2 scaling

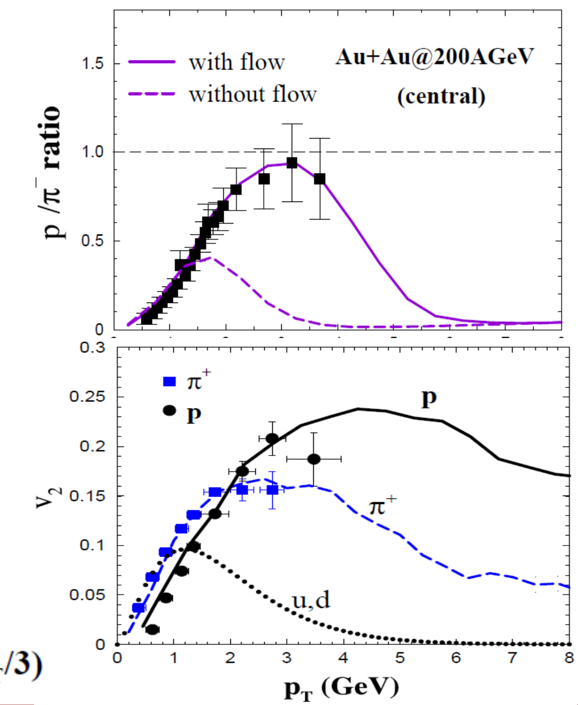

$f_M(p_T) \sim f_q(p_T/2)*f_{qbar}(p_T/2)$ VS $f_B(p_T) \sim f_q(p_T/3)*f_q(p_T/3)*f_q(p_T/3)$

Instantaneous coalescence model

❖ ICM: usually implemented only in momentum space

Oh et al., PRC79, 044905 (2009)

- with a Gaussian Wigner function, $\triangle_x$=σ~hadron radius, $\triangle_p$=1/σ

$$\frac{dN_M}{d\boldsymbol{p}_M} = g_M \frac{(2\sqrt{\pi}\sigma)^3}{V} \int d\boldsymbol{p}_1 d\boldsymbol{p}_2 \frac{dN_1}{d\boldsymbol{p}_1} \frac{dN_2}{d\boldsymbol{p}_2} \times \exp(-\boldsymbol{k}^2\sigma^2)\delta(\boldsymbol{p}_M - \boldsymbol{p}_1 - \boldsymbol{p}_2),$$

relative momentum **k** measured in meson rest frame
degeneracy $g_M=(2s_M+1)/[(2s_1+1)*3_c*(2s_2+1)*3_c]$,
e.g. $g_{D0}=1/36$, $g_{D*}=3/36=1/12$

$$\boldsymbol{k} = \frac{1}{m_1+m_2}(m_2\boldsymbol{p}_1' - m_1\boldsymbol{p}_2')$$

- for charm baryons

$$\frac{dN_B}{d\boldsymbol{p}_B} = g_B \frac{(2\sqrt{\pi})^6(\sigma_1\sigma_2)^3}{V^2} \int d\boldsymbol{p}_1 d\boldsymbol{p}_2 d\boldsymbol{p}_3 \frac{dN_1}{d\boldsymbol{p}_1} \frac{dN_2}{d\boldsymbol{p}_2} \frac{dN_3}{d\boldsymbol{p}_3} \times \exp\left(-\boldsymbol{k}_1^2\sigma_1^2 - \boldsymbol{k}_2^2\sigma_2^2\right)\delta(\boldsymbol{p}_B - \boldsymbol{p}_1 - \boldsymbol{p}_2 - \boldsymbol{p}_3),$$

$$\boldsymbol{k}_1 = \frac{1}{m_1+m_2}(m_2\boldsymbol{p}_1' - m_1\boldsymbol{p}_2'),$$

$$\boldsymbol{k}_2 = \frac{1}{m_1+m_2+m_3}[m_3(\boldsymbol{p}_1' + \boldsymbol{p}_2') - (m_1+m_2)\boldsymbol{p}_3']$$

$g_{\Lambda c}=2/216=1/108$

- By construction, only 3-mom. conserved, energy not conserved ➔ equilibrium limit challenging to reach at low p_T

HQ hadronization (III): RRM

- **Hadronization = Resonance formation** $c\bar{q} \rightarrow D$

  → ***consistent with T-matrix findings of resonance correlations towards T_c***

- **Realized by Boltzmann equation** Ravagli & Rapp,2007

$$p^{\mu}\partial_{\mu} f_M(t,\vec{x},\vec{p}) = -m\Gamma f_M(t,\vec{x},\vec{p}) + p^0\beta(\vec{x},\vec{p})$$

$$\beta(\vec{x},\vec{p}) = \int \frac{d^3p_1 d^3p_2}{(2\pi)^6} f_q(\vec{x},\vec{p}_1) f_{\bar{q}}(\vec{x},\vec{p}_2) \times \sigma(s) v_{\rm rel}(\vec{p}_1,\vec{p}_2)\delta^3(\vec{p}-\vec{p}_1-\vec{p}_2)$$

gain term

Breit-Wigner

$$\sigma(s) = g_\sigma \frac{4\pi}{k^2} \frac{(\Gamma m)^2}{(s-m^2)+(\Gamma m)^2}$$

- **Equilibrium limit** $$f_M(\vec{x},\vec{p}) = \frac{\gamma_{p,M}}{\Gamma_M} \int \frac{d^3\vec{p}_1 d^3\vec{p}_2}{(2\pi)^3} f_q(\vec{x},\vec{p}_1) f_{\bar{q}}(\vec{x},\vec{p}_2) \times \sigma_M(s) v_{\rm rel}(\vec{p}_1,\vec{p}_2)\delta^3(\vec{p}-\vec{p}_1-\vec{p}_2) \, ,$$

- **Energy conservation (finite width, not on-shell) + detailed balance**

→ **equilibrium mapping between quark & meson distributions**

Generalization to 3-body RRM

- **The 1st step: $q_1(p_1) + q_2(p_2) \rightarrow$ diquark (p_{12})**

$$f_d(\vec{x},\vec{p}_{12}) = \frac{E_d(\vec{p}_{12})}{\Gamma_d m_d}\int \frac{d^3p_1 d^3p_2}{(2\pi)^3} f_1(\vec{x},\vec{p}_1) f_2(\vec{x},\vec{p}_2)\sigma_{12}(s_{12}) v_{\rm rel}^{12}(\vec{p}_1,\vec{p}_2)\delta^3(\vec{p}_{12}-\vec{p}_1-\vec{p}_2)$$

- **The 2nd step: diquark $(p_{12}) + q_3(p_3) \rightarrow$ baryon (p)**

$$\begin{aligned} f_B(\vec{x},\vec{p}) &= \frac{E_B(\vec{p})}{\Gamma_B m_B}\int \frac{d^3p_{12} d^3p_3}{(2\pi)^3} f_d(\vec{x},\vec{p}_{12}) f_3(\vec{x},\vec{p}_3)\sigma_B(s_{d3}) v_{\rm rel}^{d3}(\vec{p}_{12},\vec{p}_3)\delta^3(\vec{p}-\vec{p}_{12}-\vec{p}_3) \\ &= \frac{E_B(\vec{p})}{\Gamma_B m_B}\int \frac{d^3p_1 d^3p_2 d^3p_3}{(2\pi)^6} \frac{E_d(\vec{p}_{12})}{\Gamma_d m_d} f_1(\vec{x},\vec{p}_1) f_2(\vec{x},\vec{p}_2) f_3(\vec{x},\vec{p}_3) \\ &\times \sigma_{12}(s_{12}) v_{\rm rel}^{12}(\vec{p}_1,\vec{p}_2)\sigma_B(s_{d3}) v_{\rm rel}^{d3}(\vec{p}_{12},\vec{p}_3)|_{\vec{p}_{12}=\vec{p}_1+\vec{p}_2}\delta^3(\vec{p}-\vec{p}_1-\vec{p}_2-\vec{p}_3) \end{aligned}$$

diquark type	mass (MeV)	wave func.	charm-baryon
Scalar [u,d]	710	$\bar{3}_{\rm color}\bar{3}_{\rm flavor}0^+_{\rm spin}$	Λ_c: c[ud]
Axialvector {u,d}	909	$\bar{3}_{\rm color}6_{\rm flavor}1^+_{\rm spin}$	Σ_c: c{ud}

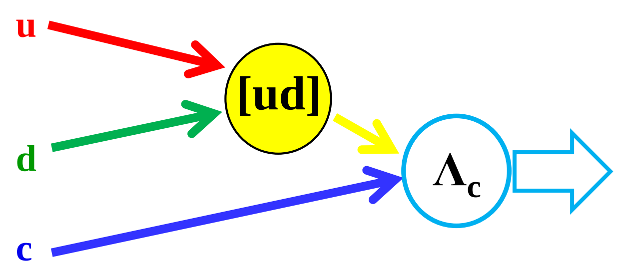

- Meson/baryon invariant spectra on hydrodynamic Cooper-Frye hypersurface at T_H=170 MeV

$$\frac{dN_{M,B}}{p_T dp_T d\phi_p dy} = \int \frac{p\cdot d\sigma}{(2\pi)^3} f_{M,B}(\vec{x},\vec{p})$$

MH & Rapp, PRL124, 042301 (2020)

RRM: equilibrium mapping

- RRM on hydrofreezeout hypersurface at T_c with $f_q^{eq}(\vec{x},\vec{p}) = g_q e^{-p\cdot u(x)/T(x)}$

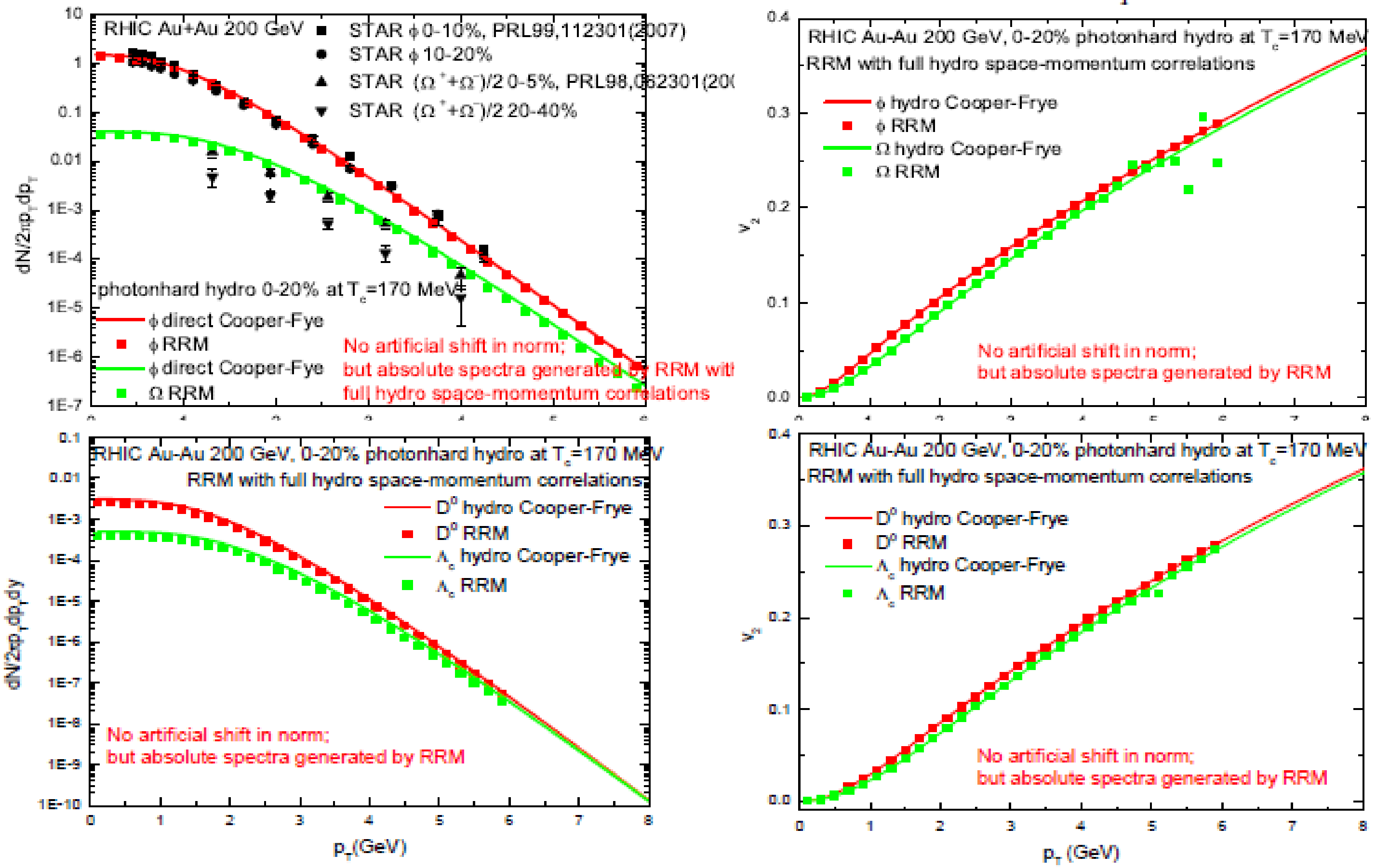

- Equilibrium mapping: ensured by 4-momentum conservation in RRM
  m_q=0.3, m_s=0.4, m_c=1.5, Γ_M~0.1 GeV, Γ_d~0.2 GeV, Γ_B~0.3 GeV

Space-momentum correlations (SMCs)

- **hydro: a manifestation of SMCs**

$$f_q^{eq}(\vec{x},\vec{p}) = g_q e^{-p\cdot u(x)/T(x)} = g_q e^{-\gamma_T(x)[m_T\cosh(y-\eta)-\vec{p}_T\cdot\vec{v}_T(x)]/T(x}$$

longitudinal boost invariance: y- η **transverse SMCs $p_T \cdot v_T$**

- **hydro-q density: low (high) p_T-q more concentrated in center (boundary)**

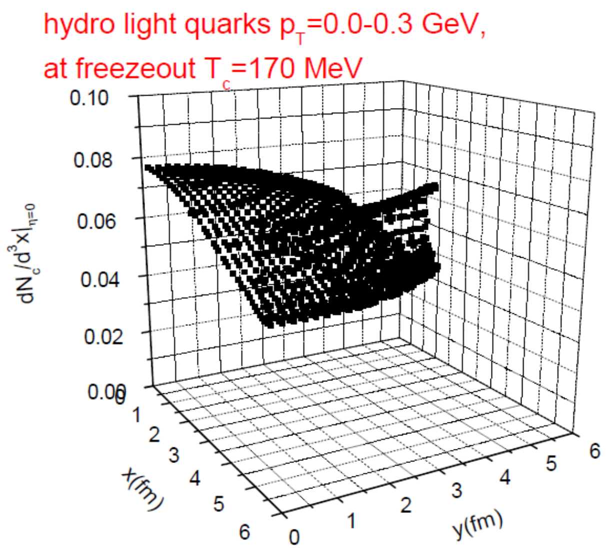

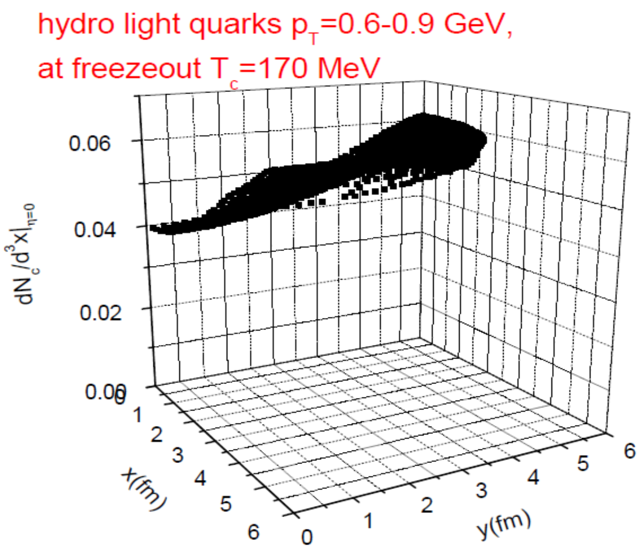

- **what if neglecting SMCs: uniformly distributed independent of p_T as usually done in conventional instantaneous coalescence models**

$$f_{c,q}(\vec{x},\vec{p}) = (2\pi)^3\frac{dN_{c,q}}{d^3\vec{x}d^3\vec{p}} = \frac{(2\pi)^3}{VE_{(\vec{p})}}\frac{dN_{c,q}}{p_T dp_T d\phi_q dy} \quad \& \quad \int p\cdot d\sigma = E(\vec{p})V$$

SMCs: Langevin charm quarks

- Langevin simulation of charm quark diffusion in a hydrodynamically expanding QGP with T-matrix charm thermalization rate
- c-quarks: low (high) p_T-c more populated in central (outer) region

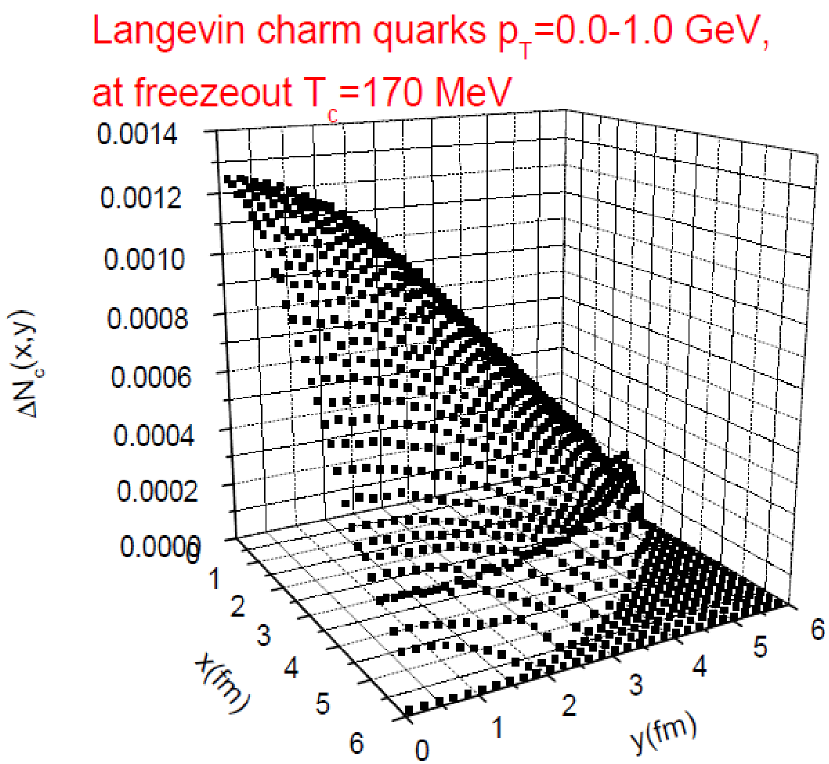

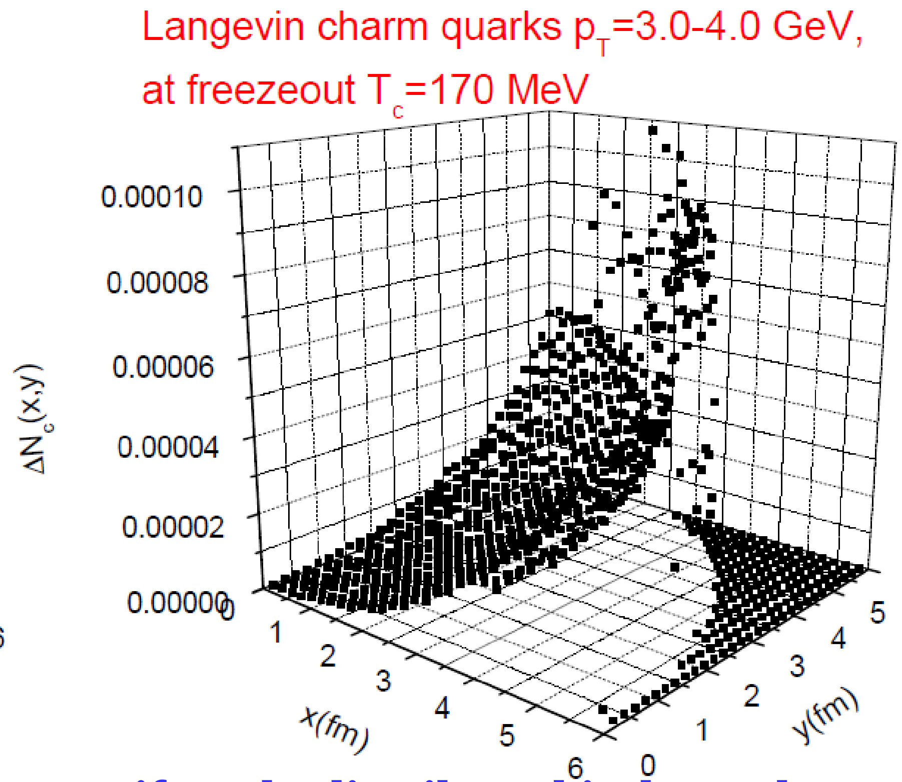

- SMCs usually neglected in ICMs: uniformly distributed independent of p_T
- what will be the role of SMCs in recombination/RRM?

Charm quark recombination probability

- No. of mesons/baryons formed from a single c-quark of rest frame p_c*

$$N_M(p_c^*) = \int \frac{d^3\vec{p}_1^{\,*}}{(2\pi)^3} g_q e^{-E(\vec{p}_1^{\,*})/T_{pc}} \frac{E_M(\vec{p}^{\,*})}{m_M \Gamma_M} \sigma(s) v_{\rm rel},$$

$$N_B(p_c^*) = \int \frac{d^3p_1 d^3p_2}{(2\pi)^6} g_1 e^{-E(\vec{p}_1)/T_c} g_2 e^{-E(\vec{p}_2)/T_c} \frac{E_d(\vec{p}_{12})}{m_d\Gamma_d} \sigma(s_{12}) v_{\rm rel}^{12}(\vec{p}_1,\vec{p}_2) \frac{E_B(\vec{p})}{m_B\Gamma_B} \sigma(s_{d3}) v_{rel}^{d3}(\vec{p}_{12},\vec{p}_{30}),$$

- Renormalizing $N_M(p_c^*)$ and $N_B(p_c^*)$ by a common factor ~4 for all charmed mesons/baryons such that $\sum_M P_{{\rm coal},M}(p_c^*=0) + \sum_B P_{{\rm coal},B}(p_c^*=0) = 1$

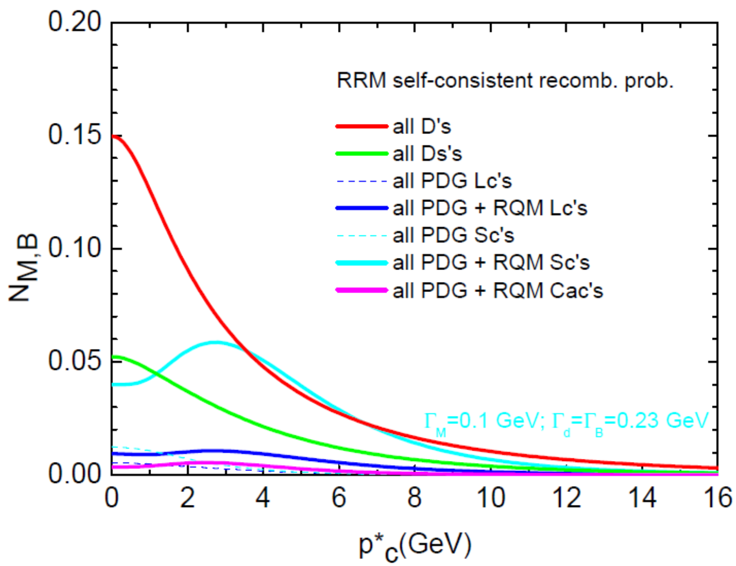

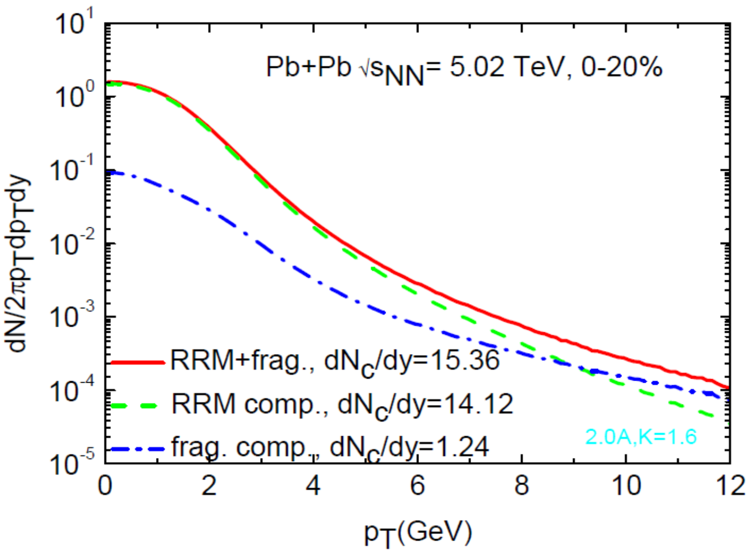

--- charm conservation separately built in, in a (e-by-e) way without spoiling the relative chemical equilibrium realized by RRM

Event-by-event Langevin-RRM simulation

- for a single Langevin c-quark, sample a/two thermal light-q distribution(s)

$$\frac{dN_M}{d\eta}|_{\eta=0} \equiv \sum_n \Delta N_M[n] = \sum_n \frac{p \cdot d\sigma(j_0)}{m_M \Gamma_M} \sigma(s) v_{\rm rel} \qquad \vec{p} = \vec{p}_{1n} + \vec{p}_c$$

$$\frac{dN_B}{d\eta}|_{\eta=0} \equiv \sum_{n_1} \sum_{n_2} \Delta N_B[n_1, n_2]$$

$$= \sum_{n_1} \sum_{n_2} \frac{p \cdot d\sigma(j_0)}{m_B \Gamma_B} \frac{E_d(\vec{p}^*_{12})}{m_d \Gamma_d} \sigma(s_{12}) v^{12}_{\rm rel}(\vec{p}^*_{1n_1}, \vec{p}^*_{2n_2}) \sigma(s_{d3}) v^{d3}_{rel}. \qquad \vec{p} = \vec{p}_{1n_1} + \vec{p}_{2n_2} + \vec{p}_c$$

- equil. mapping with large transport coeffi. checks out: SMCs incorporated

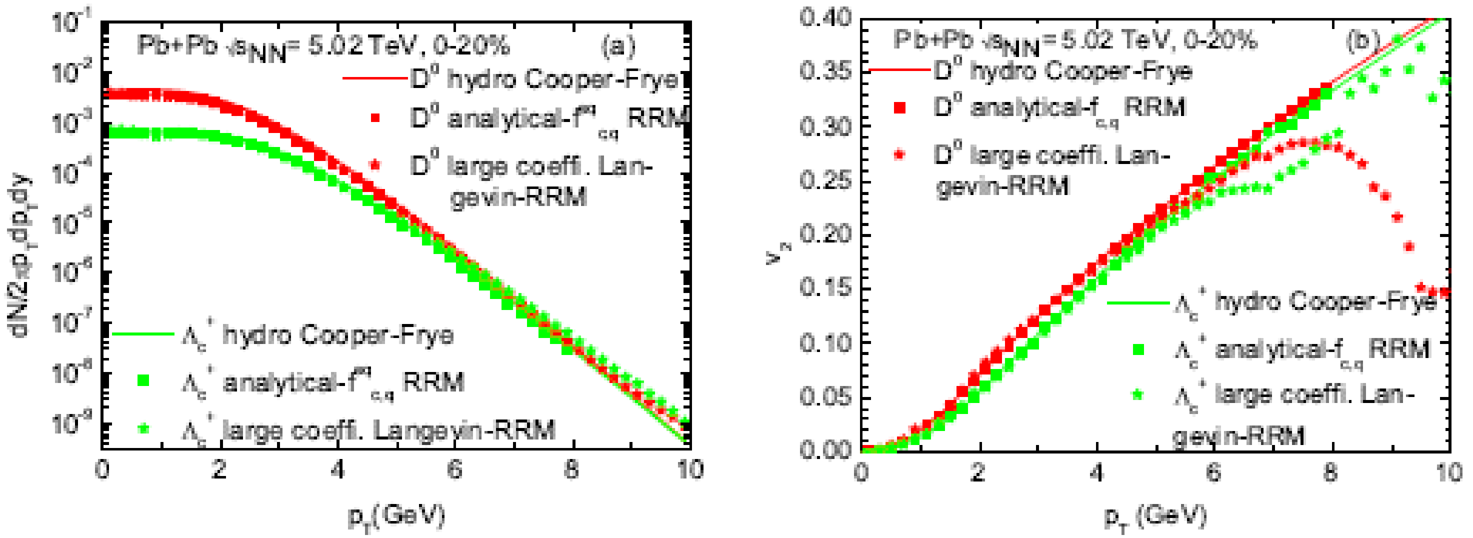

- equil. mapping : both kinetic & chemical ➔ observables come out as RRM predictions with realistic T-matrix transport coefficient

Direct D^0 & Λ_c^+ production via RRM

- Including **SMCs** makes the spectra harder & enhances the ratio Λ_c^+/D_0

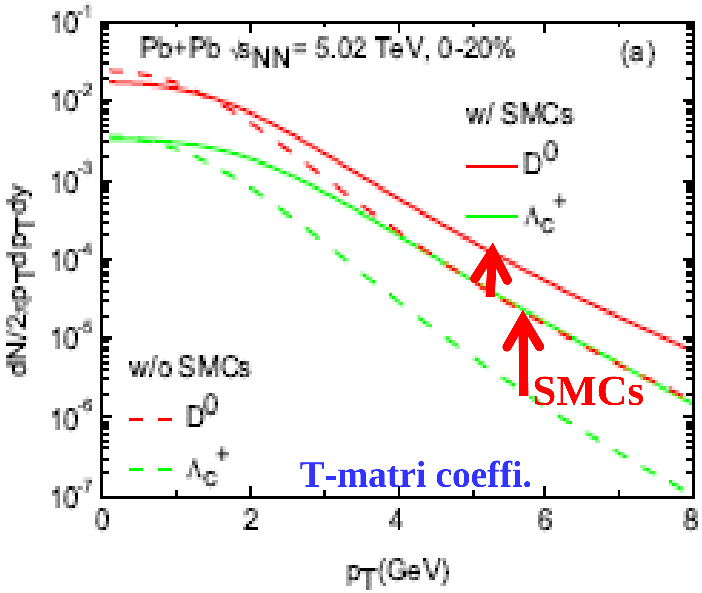

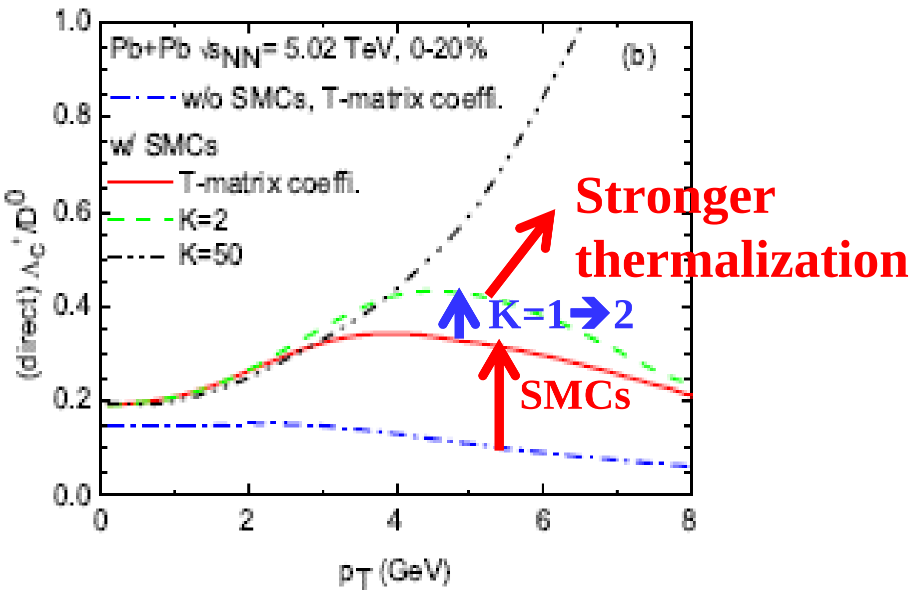

- Consider RRM formation of D^0 (3.5+0.7) & Λ_c^+ (3.0+0.6+0.6) of p_T~4.2 GeV:

  enhancement of density of light-q of p_T~ 0.6-0.7 GeV & c of p_T~3.0-3.5 GeV

$$\Delta N_{D^0}(4.2) \sim \frac{\Delta N_c(3.0-3.5)}{V_{c,\mathrm{eff}}} \cdot \frac{\Delta N_q(0.6-0.7)}{V_{q,\mathrm{eff}}} \qquad (15)$$

--- Rencombinant quark density enhanced vs w/o SMCs: $V_{eff}<V_{fb}$

$$\Delta N_{\Lambda_c^+}(4.2) \sim \frac{\Delta N_c(3.0-3.5)}{V_{c,\mathrm{eff}}} \cdot \frac{\Delta N_q(0.6-0.7)}{V_{q,\mathrm{eff}}} \cdot \frac{\Delta N_q(0.6-0.7)}{V_{q,\mathrm{eff}}}$$

--- Enhanced light-q density entering D^0 RRM only once vs twice (squared) for Λ_c^+ RRM ➔ the ratio Λ_c^+/D^0 enhanced!

Recombinant vs fragmenting spectra

- Hydro-Langevin-RRM(+fragmentation): for all charm-mesons/baryons
  ➔ higher states decay into ground state D^0 , D^+ , D_s^+ , Λ_C^+

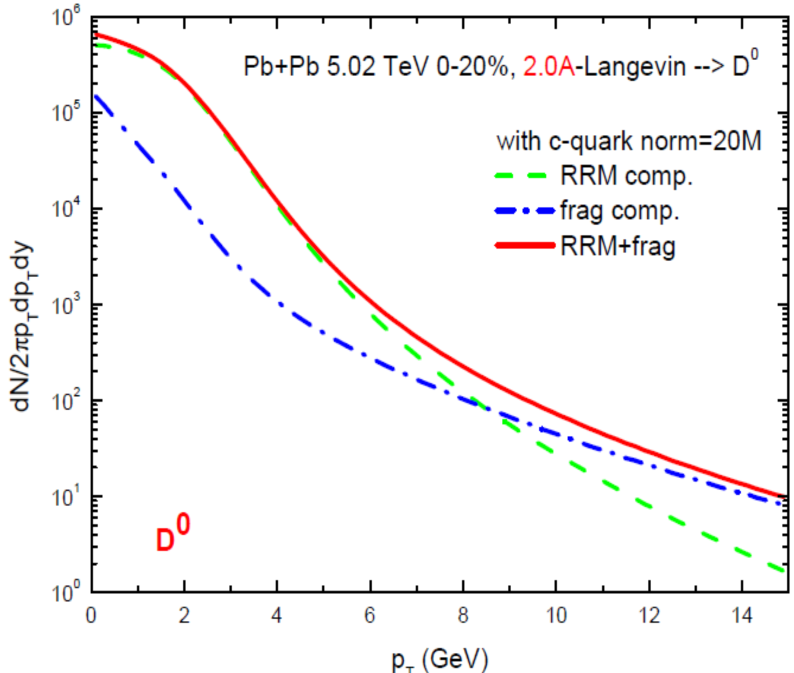

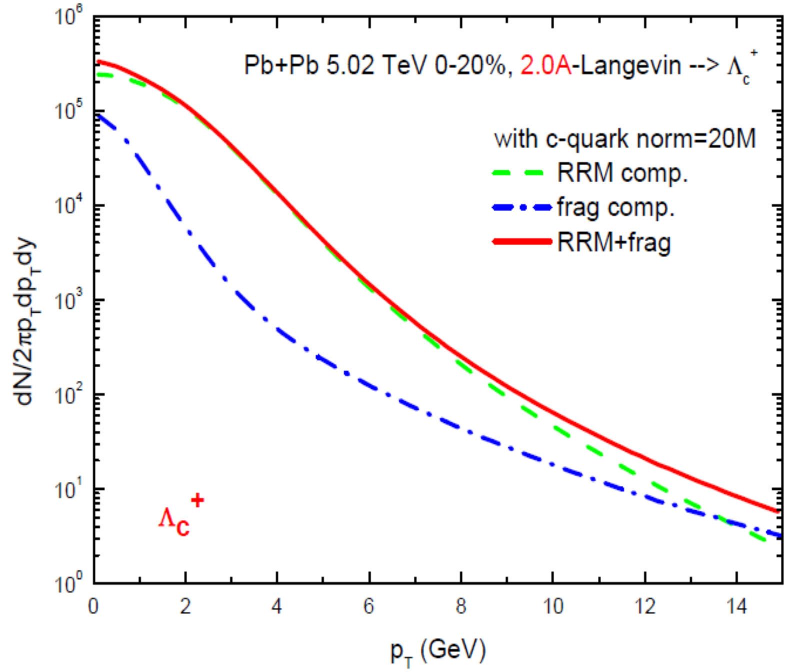

- SMCs extend the recombinant component toward (quite) high p_T; RQM augmented higher states' RRM spectra even harder (also thanks to SMCs) ➔ RRM & frag. cross at p_T ~8.5 (13) GeV for D^0 (Λ_C^+)

- Helpful for large total v_2 (weighted between RRM vs frag. components)

HQ hadronization (IV): fragmentation

- charm quarks that are not consumed via recombination ($P_{coal}(p_{c^*})<1$ is a decreasing function toward high p_{c^*}) go to independent fragmentation

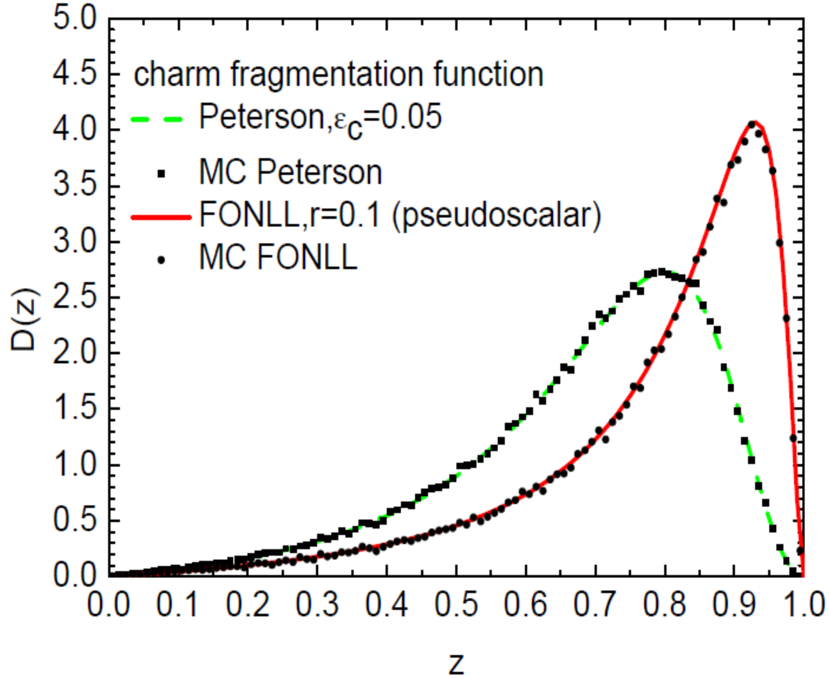

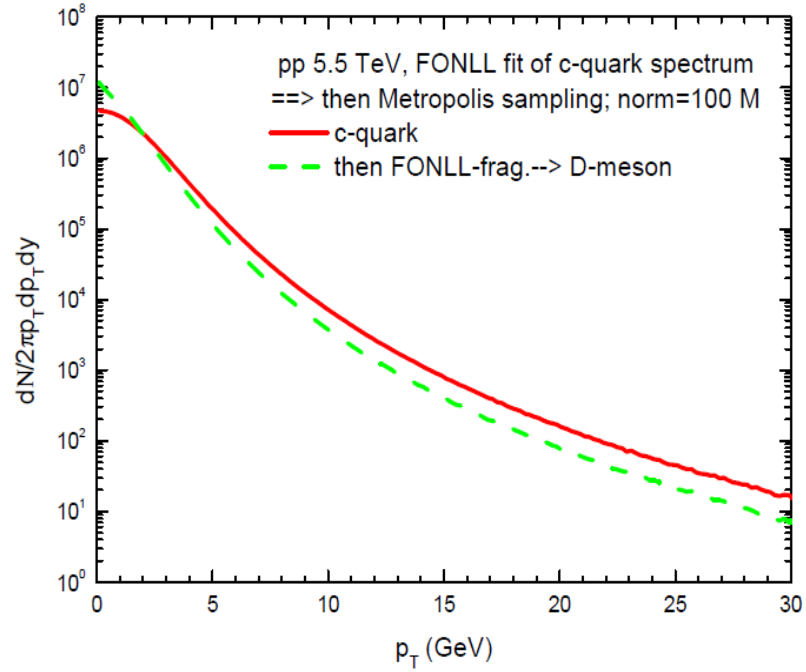

- $z = p_{TH}/p_{Tc}$

$$D_{c\to H}(z) = N_H \frac{rz(1-z)^2}{[1-(1-r)z]^6}[(6-18(1-2r)z + (21-74r+68r^2)z^2 - 2(1-r)(6-19r+18r^2)z^3 + 3(1-r)^2(1-2r+2r^2)z^4] \,,$$

$$r_M/r_{D^0} = ((m_M - m_c)/m_M)/((m_{D^0} - m_c)/m_{D^0})$$

$$r_B/r_{\Lambda_c^+} = ((m_B - m_c)/m_B)/((m_{\Lambda_c^+} - m_c)/m_{\Lambda_c^+})$$

Recombination vs fragmentation

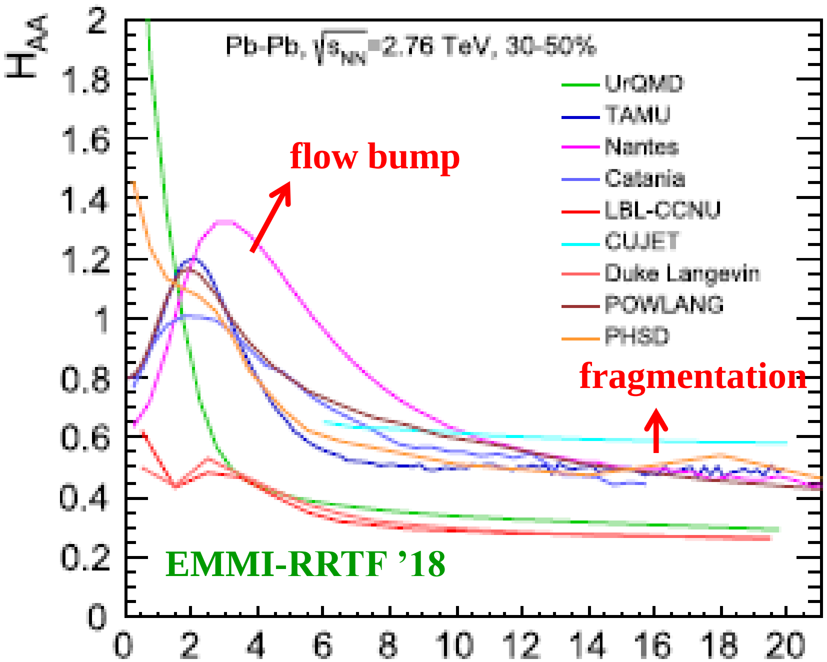

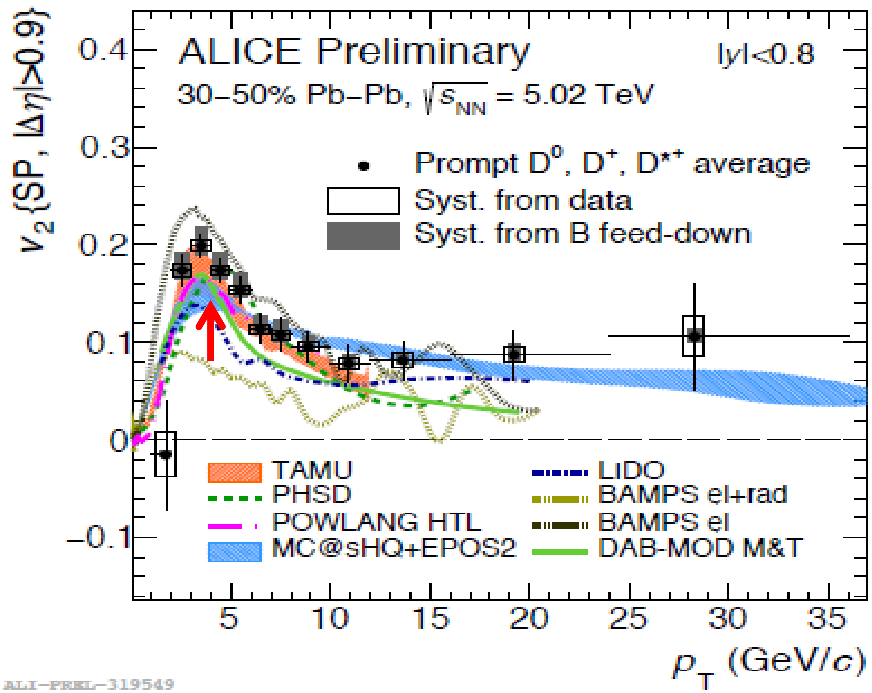

$$H_{\mathrm{AA}}(p_T, p_t = p_T) = \frac{\mathrm{d}N_D/\mathrm{d}p_T}{\mathrm{d}N_c/\mathrm{d}p_t} = \frac{\mathrm{d}N_D^{\mathrm{coal}}/\mathrm{d}p_T + \mathrm{d}N_D^{\mathrm{frag}}/\mathrm{d}p_T}{\mathrm{d}N_c/\mathrm{d}p_t}$$

- Recombination dominant at low p_T: adding flow from light quark to charm quark ➔ flow bump in the H_{AA} and also in R_{AA} & v_2 increased from c to D
- Fragmentation dominant at high p_T: p_T shift from c to D

D-meson R_{AA} & v_2: extracting $\mathcal{D}_s(2\pi T)$

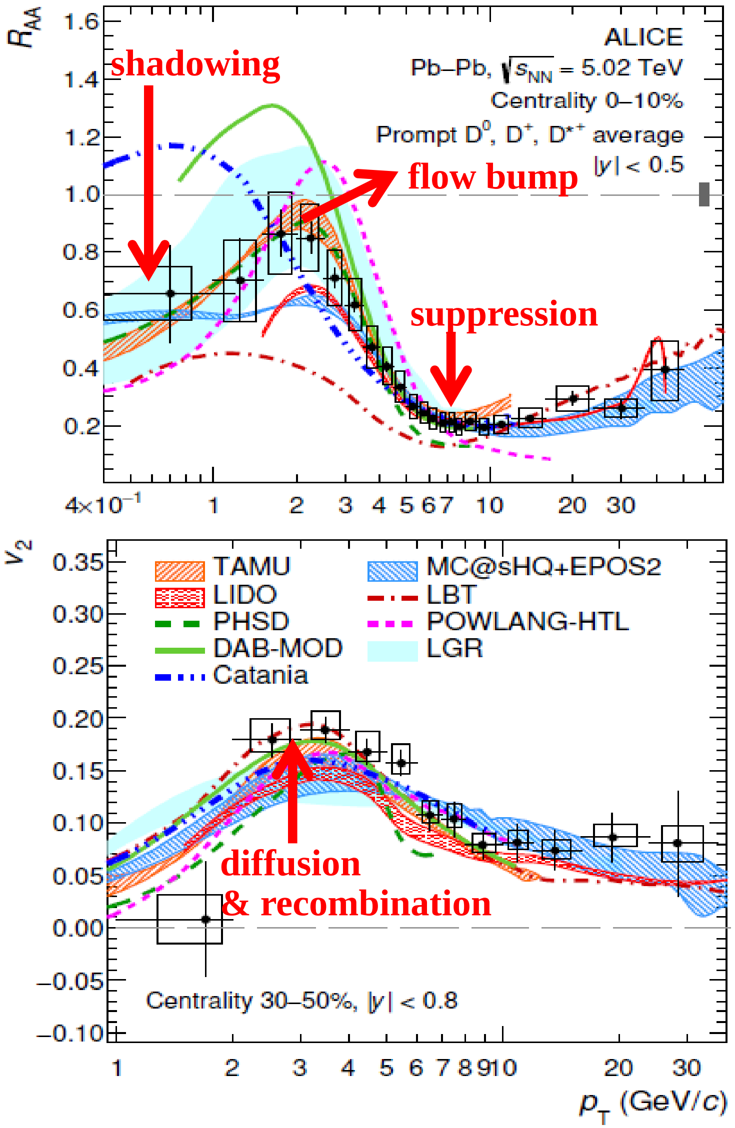

ALICE, JHEP01(2022)174; PLB 813(2021)136054

Model	χ^2/ndf R_{AA}	χ^2/ndf v_2
Catania [6, 7]	143.8/30	14.0/8
DAB-MOD [9]	234.1/30	9.8/6
LBT [10, 11]	411.8/30	15.8/12
LIDO [13]	46.4/26	62.0/11
LGR [12]	9.2/30	15.5/11
MC@sHQ+EPOS2 [8]	56.6/30	5.7/12
PHSD [5]	294.7/30	19.6/11
POWLANG-HTL [3, 4]	468.6/30	13.5/8
TAMU [2]	30.2/30	8.15/9

- models with $\chi^2/\mathrm{ndf} < 5$ (2) for R_{AA} (v_2)
  ➔ $\mathcal{D}_s(2\pi T)$=1.5-4.5 near T_c
- caveat: also affected by hadronization, hydro, hadronic phase

Charm hadro-chemistry: Λ_c/D^0

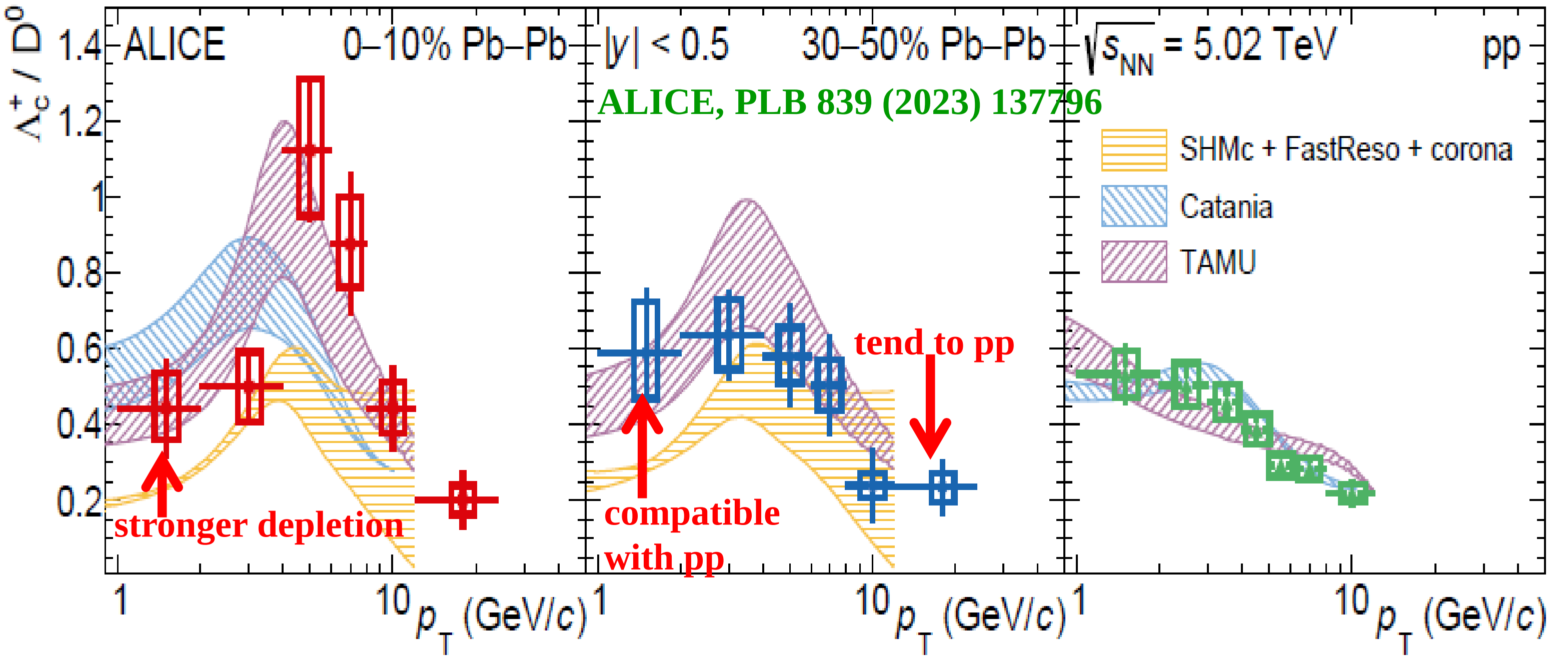

- Catania: instantaneous coalescence + fragmentation **Plumari et al. '18**
- SHMc: hydrodynamic blast wave spectrum on PDG-only baryons + corona pp **Andronic et al. '21**
- TAMU: RQM charm-baryons + RRM w/ SMCs
  integrated ratio compatible with pp **MH & Rapp '20**

p_T-integrated Λ_c/D^0 compatible with pp → kinematic redistribution in p_T in AA

Charm hadro-chemistry: D_s/D^0

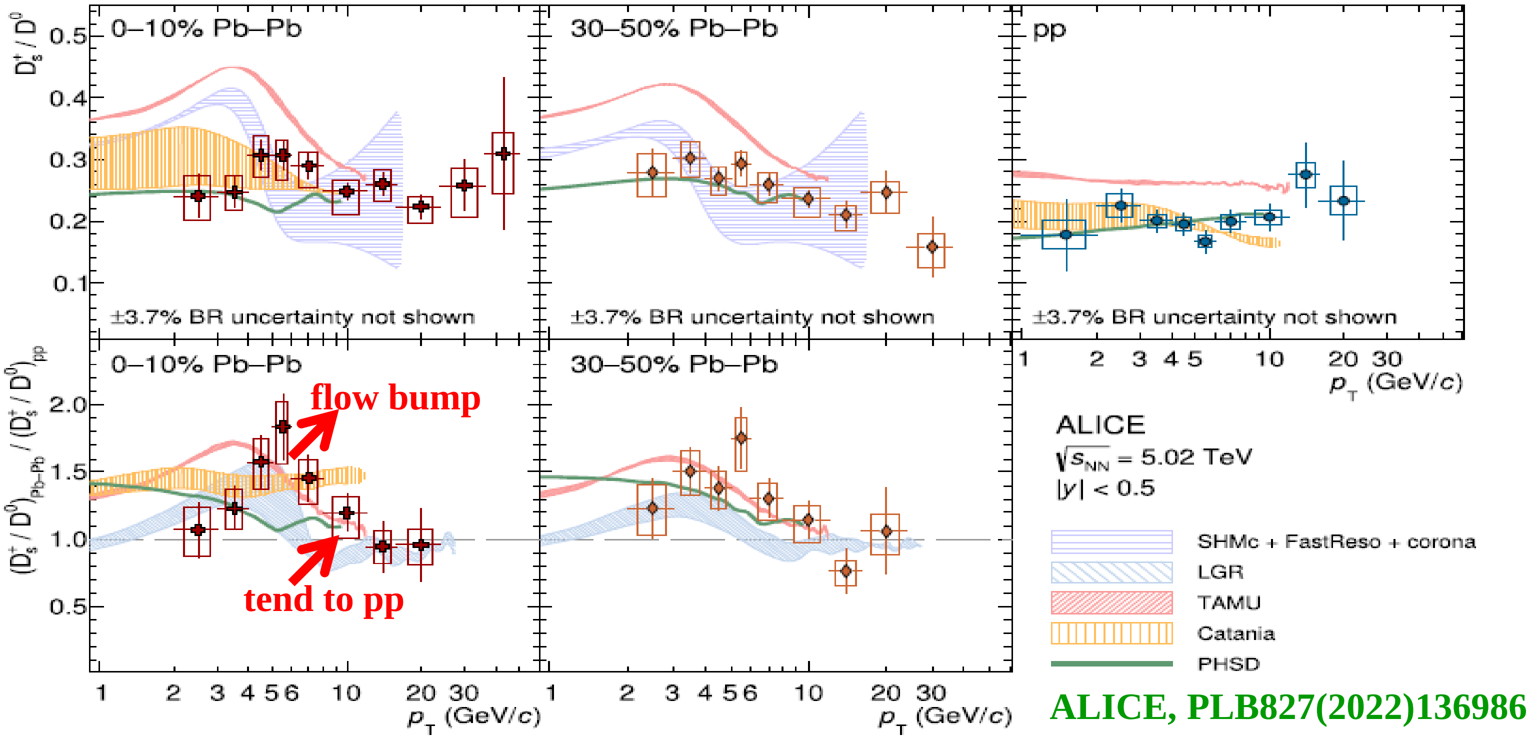

ALICE, PLB827(2022)136986

- low p_T: enhancement due to charm recombination in a strangeness-equilibrated QGP reproduced by Cantania & PHSD; overestimated by TAMU in both pp and PbPb
- high p_T: tending to pp value as fragmentation takes over
- flow bump due to recombination with flowing s-quark heavier than u/d, predicted by TAMU (RRM w/ SMCs) & SHMc (hydro blastwave spectrum)

Flavor dependence: charm vs bottom

nonprompt D (← B) R_{AA} , ALICE:2202.00815

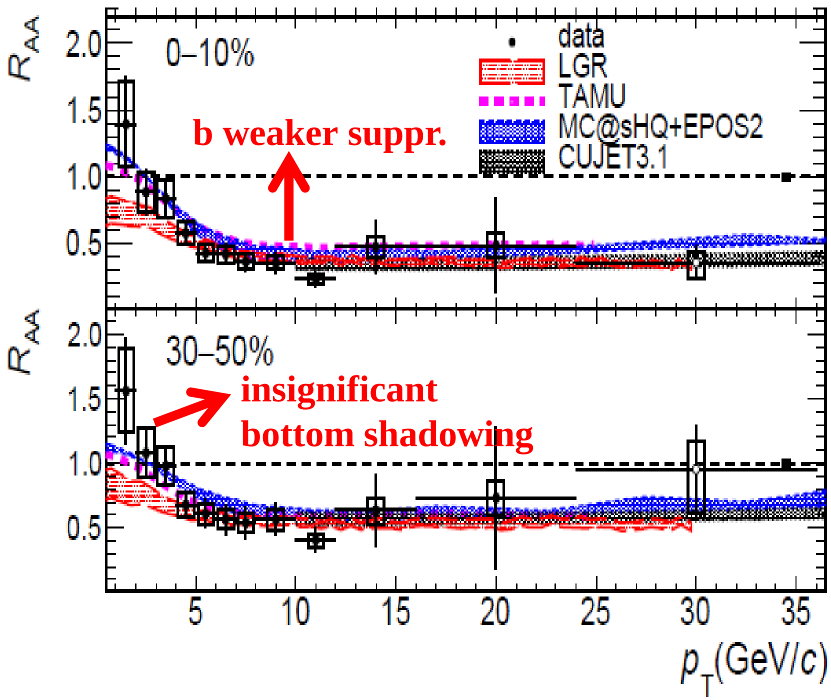

nonprompt-to-prompt D-meson R_{AA} ratio

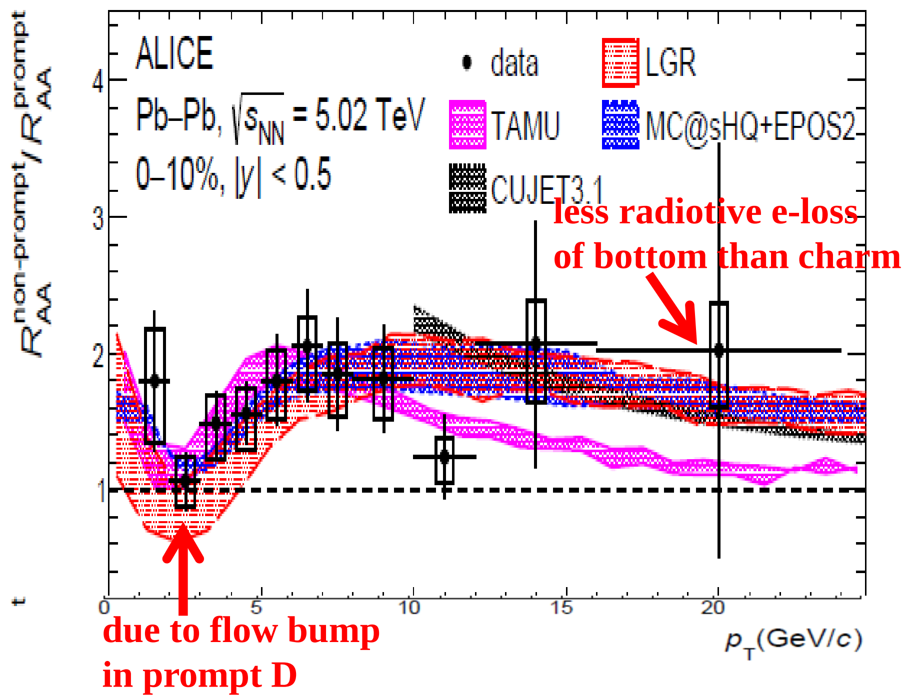

❖ x3 mass: b-quark longer thermalization time at low p_T than charm
less flow added to b from recombination with u/d/s

❖ high p_T>15 GeV: b-quark less radiative e-loss ← stronger "dead cone"

Bottom hadrochemistry: pp vs PbPb

- Statistical hadronization model with RQM-augmented b-hadrons
  + fragmentation + decay simulations
  ➔ baseline for PbPb

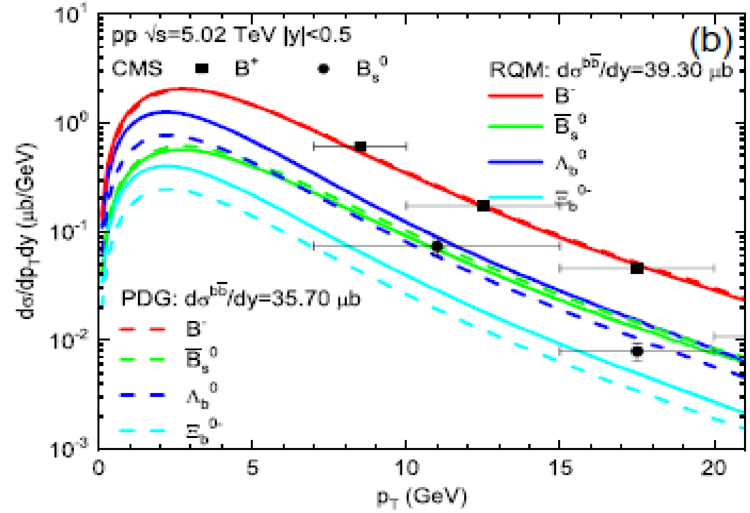

- Bottom hadrochemistry: pp vs PbPb

MH & Rapp, PRL131, 012301 (2023)

enhancement of B_s/B at low p_T: b coupled to equilibrated strangess via recombination
enhancement of baryon-to-meson at intermediate p_T: 3-body recombination with flow

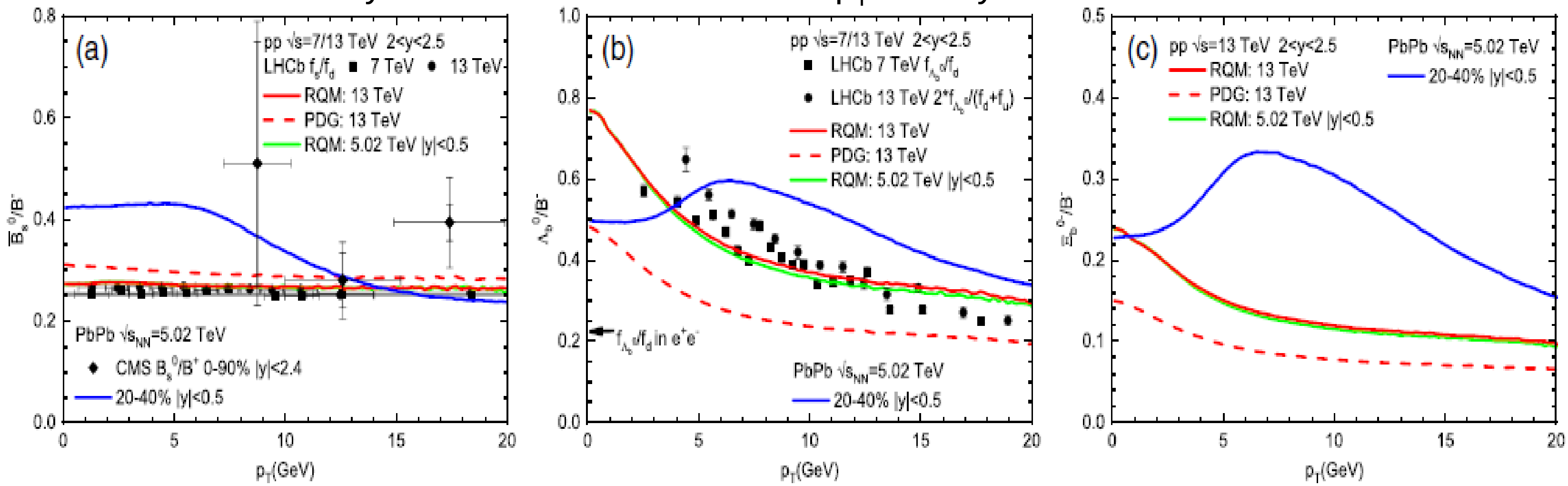

Bottom hadrons nuclear modification factor

- R_{AA} for ground state b-hadrons: hierarchy of flow effects and suppression driven by their quark content

$$R_{AA}(p_T) = \frac{dN^{AA}/dp_T dy}{< T_{AA} > d\sigma^{pp}/dp_T dy}$$

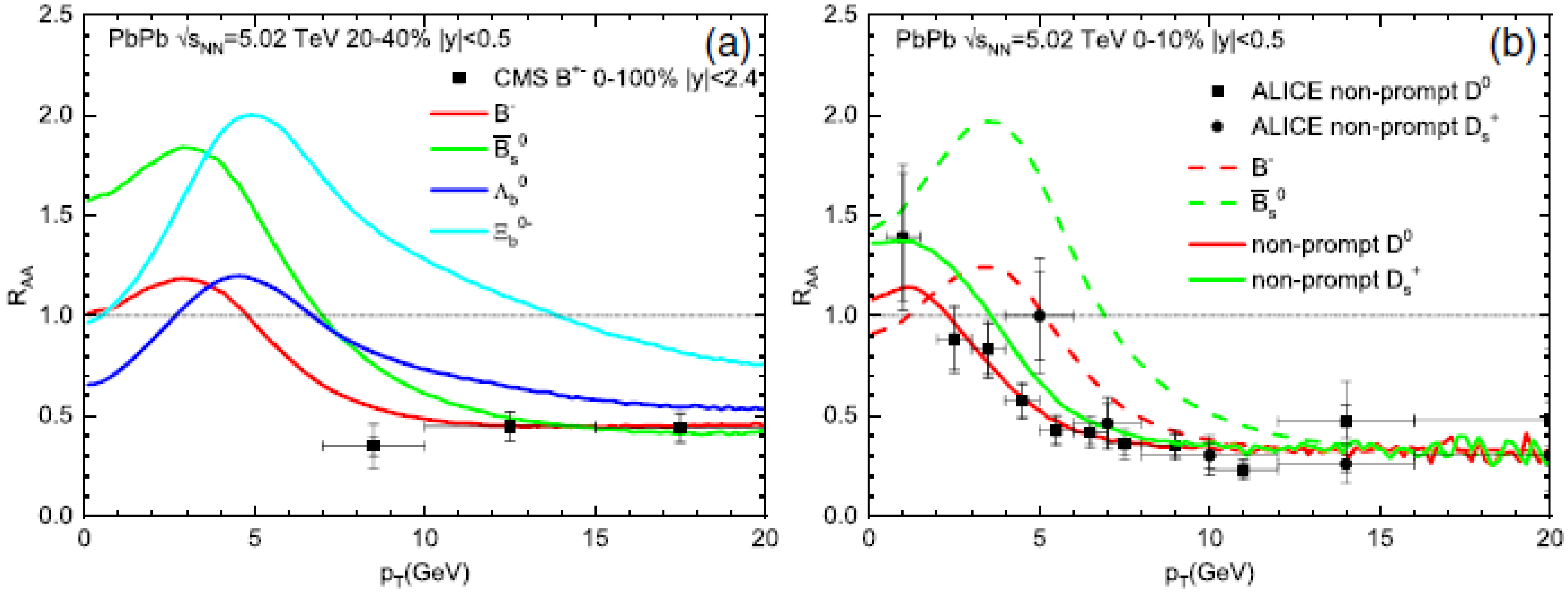

MH & Rapp, PRL131, 012301 (2023)

- Bs: b-quark coupled to equilibrated strangeness via recombination
  Λb: 3-body baryon recombination, RRM with SMCs
  Ξb: combining two-fold role of being baryon + containing a s-quark
- Non-prompt D^0 & Ds: weak decays of all b-hadrons via PYTHIA8